Photons in the presence of parabolic mirrors

R. Gutiérrez-Jáuregui[1] and R. Jáuregui[2,*]

[1]*The Dodd-Walls Centre for Photonic and Quantum Technologies, Department of Physics, University of Auckland, Private Bag 92019, Auckland, New Zealand*

[2]*Instituto de Física, Universidad Nacional Autónoma de México, Apartado Postal 20-364, 01000 Ciudad de México, Mexico*

(Received 30 April 2018; published 4 October 2018)

We present a vectorial analysis of the behavior of the electromagnetic field in the presence of boundaries with parabolic geometry. The relevance of the use of symmetries to find explicit closed expressions for the electromagnetic fields is emphasized. Polarization and phase related angular momenta of light have an essential role in the proper definition of the generator $\mathfrak{A}_3$ of a symmetry transformation that distinguishes the parabolic geometry. Quantization of the electromagnetic field in terms of the resulting elementary modes is performed. The important case of a boundary defined by an ideal parabolic mirror is explicitly worked out. The presence of the mirror restricts the eigenvalues of $\mathfrak{A}_3$ available to the electric and magnetic fields of a given mode via compact expressions. Modes previously reported in the literature are particular cases of those described in this work.

DOI: 10.1103/PhysRevA.98.043808

I. INTRODUCTION

Due to its focusing properties, the parabola of revolution has been considered an optimal geometry to build mirrors and lenses since classical antiquity. Parabolic mirrors are usually designed under conditions that allow a ray description of the relevant electromagnetic (em) modes. Recently, there have been attempts to make a detailed description beyond this approximation, introducing vectorial classical [1] and quantum [2] properties of the electromagnetic field in the presence of parabolic boundaries; a motivation being the possibility of optimizing the coupling of single atoms to single photons. The basic idea behind this optimization is that the processes of elastic scattering [3,4] and absorption [5,6] of a photon by a single atom increase their efficiencies for incident light that spatially resembles the natural mode of the atomic transition, which usually corresponds to an electric dipole wave. It has been shown that a deep parabolic mirror can focus a radially polarized doughnut mode to a field that is nearly linearly polarized along the optical axis and, close to the focus of the parabola, is similar to the dipole field [7–9]. Experiments working on this direction have led to a better understanding of the interaction between photons and atomic systems under controlled conditions with remarkable results [10–12].

Previous analysis of the em field in the presence of parabolic boundaries, however, have been limited by mathematical difficulties in finding a complete set of elementary modes that fulfill both Maxwell equations and the adequate boundary conditions. As a consequence, important properties like space dependencies of the polarization are not fully understood. Nevertheless, these works have shown that particular em modes in the presence of ideal parabolic mirrors would exhibit several interesting properties. For instance, a WKB study of the dynamics within a parabolic cavity indicate that the waves without optical vortices should be robust with respect to small geometrical deformations of the cavity, while those exhibiting optical vortices could be unstable and even give rise to optical chaos [1].

In this work, we present a detailed description of the electromagnetic vectorial field in parabolic geometries that surpasses the problems mentioned above. We construct a complete set of modes that satisfy Maxwell equations and incorporate the underlying symmetries explicitly. These modes could allow a clearer description of experimental arrays involving parabolic boundaries, since they can be used to explore properties that cannot be accessed through previous descriptions. We also make a proper quantization of the em field in terms of the classical Maxwell modes; this provides an extended framework for the studies mentioned above regarding the interaction between light and matter under controlled conditions. We illustrate the relevance of this approach by working out in detail the paradigmatic configuration of the em field in the presence of an ideal parabolic mirror.

In the next section we revisit the characteristics of scalar waves in parabolic coordinates. Following Boyer *et al.* [13], the generators of the natural symmetries are identified, as well as the angular spectrum of the scalar modes. In Sec. III, we obtain the solutions of the Maxwell equations. The em modes are written in terms of vector Hertz potentials $\boldsymbol{\pi}$ with components that are, in turn, written in terms of the scalar modes. The $\boldsymbol{\pi}$ modes are chosen to yield electric $\mathbf{E}$ and magnetic $\mathbf{B}$ fields that are eigenvectors of the generators of the mentioned symmetries with the same eigenvalues; a key point is that the generators of the adequate transformations act now on the *vector* em fields. Intrinsic and orbital angular momenta of light have an essential role in the proper definition of the generator $\hat{\mathfrak{A}}_3$ of a symmetry transformation that distinguishes the parabolic geometry. The effect of an ideal parabolic mirror over the em field is considered in Sec. IV. The boundary restricts the eigenvalues of $\hat{\mathfrak{A}}_3$ available to the $\mathbf{E}$ and $\mathbf{B}$ of a given

*rocio@fisica.unam.mx

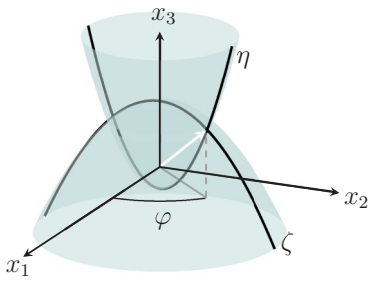

FIG. 1. Parabolic coordinates $\{\zeta, \eta, \varphi\}$. Surfaces of constant ζ (η) correspond to downward (upward) paraboloids of revolution about the x_3 axis with φ the azimuth angle. The foci of the paraboloids are located at the origin. The focal length of each downward (upward) paraboloid is twice the coordinate ζ (η).

mode via compact expressions. The modes that were worked out before are contained within the set of modes we get in this paper. The elementary modes we find are orthogonal and can be normalized according to the Einstein prescription. In this way the quantum em field operators are constructed.

II. SCALAR PARABOLIC MODES

The parabolic coordinates are defined by

$$x_1 = \sqrt{\zeta\eta}\cos\varphi, \quad x_2 = \sqrt{\zeta\eta}\sin\varphi, \quad x_3 = \tfrac{1}{2}(\zeta - \eta) \tag{1}$$

with

$$0 \leqslant \zeta < \infty, \quad 0 \leqslant \eta < \infty, \quad 0 \leqslant \varphi < 2\pi; \tag{2}$$

they are displayed in Fig. 1. In Appendix A, explicit expressions for the scale factors h_ζ, h_η, and h_φ, as well as the unitary parabolic vectors $\mathbf{e}_\zeta$, $\mathbf{e}_\eta$, and $\mathbf{e}_\varphi$ in terms of the Cartesian basis $\{\mathbf{e}_1, \mathbf{e}_2, \mathbf{e}_3\}$ are given.

In parabolic coordinates, the equation for a wave that propagates with velocity c and frequency ω,

$$\boldsymbol{\nabla}^2\Psi(\zeta,\eta,\varphi) = \frac{\omega^2}{c^2}\Psi(\zeta,\eta,\varphi) \tag{3}$$

$$= \frac{4}{\zeta+\eta}\left[\frac{\partial}{\partial\zeta}\zeta\frac{\partial}{\partial\zeta} + \frac{\partial}{\partial\eta}\eta\frac{\partial}{\partial\eta}\right]\Psi + \frac{1}{\zeta\eta}\frac{\partial^2\Psi}{\partial\varphi^2}, \tag{4}$$

is separable. As a consequence, the expression of any scalar wave can always be written as a linear combination of the elementary solutions,

$$\Psi(\zeta,\eta,\varphi) = \frac{1}{\sqrt{\bar\zeta\,\bar\eta}}\Upsilon(\bar\zeta)\Theta(\bar\eta)\Phi(\varphi), \quad \bar\zeta = \zeta\frac{\omega}{c}, \quad \bar\eta = \eta\frac{\omega}{c}, \tag{5}$$

given by a product of three functions that satisfy the equations

$$\Phi(\varphi) = \frac{1}{\sqrt{2\pi}}e^{im\varphi}, \tag{6}$$

$$\frac{d^2\Upsilon}{d\bar\zeta^2} + \left[\frac{1}{4} + \frac{\kappa}{\bar\zeta} + \frac{1/4-(m/2)^2}{\bar\zeta^2}\right]\Upsilon = 0, \tag{7}$$

$$\frac{d^2\Theta}{d\bar\eta^2} + \left[\frac{1}{4} - \frac{\kappa}{\bar\eta} + \frac{1/4-(m/2)^2}{\bar\eta^2}\right]\Theta = 0, \tag{8}$$

connected through the separation parameters m and κ. According to Eq. (6) for $\varphi \in [0, 2\pi)$, i.e., for a full paraboloid, m must be an integer. Solutions of the latter two equations can be written in terms of the Whittaker functions $M_{i\kappa,\mu}$ and $W_{i\kappa,\mu}$ of imaginary argument [14],

$$\begin{aligned} &z^{-1/2}M_{i\kappa,m/2}(iz) \\ &\quad = c_{\kappa,m}z^{m/2}e^{-iz/2}M[(m+1)/2 - i\kappa, 1+m, iz], \\ &z^{-1/2}W_{i\kappa,m/2}(iz) \\ &\quad = h_{\kappa,m}z^{m/2}e^{-iz/2}U[(m+1)/2 - i\kappa, 1+m, iz]. \end{aligned} \tag{9}$$

The hypergeometric function $M(a,b,z)$ is entire in a and z, while $U(a,b,z)$ has a branch point in $z=0$; therefore, in general, κ could take complex values with restrictions determined by the physical system under consideration as will be exemplified below.

For the interior problem, well-behaved solutions of Eqs. (7) and (8) are given by $M_{i\kappa,\mu}$, so that the scalar wave solutions take the form

$$\Psi(\zeta,\eta,\varphi) = \sum_{\kappa,m} a_{\kappa,m}e^{im\varphi}V_{\kappa,|m|}(\omega\zeta/c)V_{-\kappa,|m|}(\omega\eta/c), \tag{10}$$

where the notation

$$V_{\kappa,m}(z) = z^{|m|/2}e^{-iz/2}M\left(\frac{|m|+1}{2} - i\kappa, |m|+1; iz\right) \tag{11}$$

has been introduced. Notice that $\Psi(\zeta,\eta,\varphi)$ will be even (odd) under the parity transformation $x_3 \to -x_3$—which corresponds to $\zeta \leftrightarrow \eta$— if $a_{\kappa,m} = a_{-\kappa,m}$ ($a_{\kappa,m} = -a_{-\kappa,m}$).

The functions $V_{\kappa,m}$ satisfy the relations (valid in general for $m \geqslant 1$)

$$\sqrt{z}V_{\kappa,m-1}(z) = d_+V_{\kappa-i/2,m}(z) + d_-V_{\kappa+i/2,m}(z), \tag{12}$$

$$\sqrt{z}V_{\kappa,m+1}(z) = -i(m+1)[V_{\kappa+i/2,m}(z) - V_{\kappa-i/2,m}(z)], \tag{13}$$

$$\partial_z V_{\kappa\pm i/2,m}(z) = \left(\pm\frac{i}{2} \mp \frac{i\kappa}{z}\right)V_{\kappa\pm i/2,m}(z) + \frac{m}{z}d_\pm V_{\kappa\mp i/2,m}(z), \tag{14}$$

$$\left[\frac{2}{m}\partial_z\sqrt{z} + \frac{1}{\sqrt{z}}\right]V_{\kappa,m+1}(z) = \frac{m+1}{m}[V_{\kappa+i/2,m}(z) + V_{\kappa-i/2,m}(z)], \tag{15}$$

$$\left[\frac{2}{m}\partial_z\sqrt{z} - \frac{1}{\sqrt{z}}\right]V_{\kappa,m-1}(z) = \frac{i}{m}[d_-V_{\kappa+i/2,m}(z) - d_+V_{\kappa-i/2,m}(z)], \tag{16}$$

with

$$d_\pm = \frac{1}{2} \pm i\frac{\kappa}{m}. \tag{17}$$

Using Kummer transformation,

$$M(a,b,z) = e^zM(b-a,b,-z), \tag{18}$$

it can be directly shown that

$$V_{\kappa-i/2,m}(x) = V^*_{\kappa+i/2,m}(x) \tag{19}$$

for κ and x real variables.

In the case of κ a real number and m an odd natural number,

$$V_{\kappa,m}(z) = \frac{2\Gamma(m+1)e^{\pi\kappa/2}}{\left|\Gamma\left(\frac{m+1}{2}+i\kappa\right)\right|}\frac{1}{\sqrt{z}}F_{(m-1)/2}\left(\kappa;\frac{z}{2}\right) \tag{20}$$

with $F_{(m-1)/2}$ a real valued Coulomb function. These functions are well studied due to their relevance in the context of the Dirac wave function of an electron in a Coulomb potential [14], and as such, provide a guideline for properties-e.g., limiting forms—that will be useful in forthcoming sections.

Symmetries, angular spectrum, and normalization of the scalar modes

The symmetries behind the separability of the wave equation in parabolic coordinates [13] are induced by the generator of rotations along the x_3 axis,

$$\widehat{L}_3, \tag{21}$$

and the operator

$$\tfrac{1}{2}[\{\widehat{L}_1, \widehat{P}_2\} - \{\widehat{L}_2, \widehat{P}_1\}], \tag{22}$$

that results from the subtraction of the symmetrized product of the generator of rotations along the x_1 axis and translations along the x_2 axis, and the symmetrized product of the generator of rotations along the x_2 axis and the translations along the x_1 axis; both generators act on the scalar wave field. The latter operator is the third component of the operator obtained from the product of the angular and linear momenta operators, $(\widehat{\boldsymbol{L}}\times\widehat{\boldsymbol{P}}-\widehat{\boldsymbol{P}}\times\widehat{\boldsymbol{L}})/2$, which is the kinetic part of the well studied Runge-Lenz vector that, in turn, is the generator of a peculiar symmetry associated to a charged particle in the presence of the Coulomb potential [15]; its connection to a parabolic description of such a system is made explicit in Ref. [16].

While in the coordinate representation the expression of operator Eq. (22) is cumbersome, in the wave vector representation it is quite simple, as can be directly derived from the equations

$$\begin{aligned}
\frac{c}{\omega}\mathbf{k} &= \sin\theta_k\cos\varphi_k\mathbf{e}_1 + \sin\theta_k\sin\varphi_k\mathbf{e}_2 + \cos\theta_k\mathbf{e}_3,\\
-i\widehat{L}_1 &\to +\sin\varphi_k\partial_{\theta_k} + \cos\varphi_k\mathrm{ctan}\theta_k\partial_{\varphi_k},\\
-i\widehat{L}_2 &\to -\cos\varphi_k\partial_{\theta_k} + \sin\varphi_k\mathrm{ctan}\theta_k\partial_{\varphi_k},\\
-i\widehat{L}_3 &\to -\partial_{\varphi_k}.
\end{aligned} \tag{23}$$

Notice that the structure of $\mathbf{k}$ is necessary for the fulfillment of Helmholtz equation in the wave-vector space. This yields

$$\tfrac{1}{2}[\{\widehat{L}_1, \widehat{P}_2\} - \{\widehat{L}_2, \widehat{P}_1\}] \to i\sin\theta_k\partial_{\theta_k} + i\cos\theta_k, \tag{24}$$

when the unit of length $|\mathbf{k}|^{-1} = c/\omega$ is taken for waves with frequency ω. Notice that $i\sin\theta_k\partial_{\theta_k} + i\cos\theta_k = i\partial_{\theta_k}\sin\theta_k$ measures variations on the angle θ_k of the scalar wave, taking into account the scale factor that projects the wave vector to its component perpendicular to the x_3 axis. The normalized eigenstates of both symmetry operators, Eqs. (21) and (24),

$$\begin{aligned}
\widehat{L}_3 f_{\kappa,m} &= m f_{\kappa,m},\\
\tfrac{1}{2}[(\{\widehat{L}_1, \widehat{P}_2\} - \{\widehat{L}_2, \widehat{P}_1\})]f_{\kappa,m} &= 2\kappa f_{\kappa,m},
\end{aligned} \tag{25}$$

are given by the expression

$$f_{\kappa,m}(\theta_k,\varphi_k) = \frac{[\tan(\theta_k/2)]^{-i2\kappa}}{\sin\theta_k}\frac{e^{im\varphi_k}}{2\pi}. \tag{26}$$

The parabolic symmetry operator, Eq. (24), is Hermitian in the domain of $f_{\kappa,m}$ functions with κ a real number. These functions satisfy the orthonormality condition

$$\int_{\mathbb{S}_2^{(k)}} f^*_{\kappa',m'}(\theta_k,\varphi_k)f_{\kappa,m}(\theta_k,\varphi_k)d\Omega_k = \delta(2\kappa'-2\kappa)\delta_{m,m'}. \tag{27}$$

Equations (25) give a geometric interpretation—and can induce a dynamical interpretation—to the separation variables m and κ. The eigenfunctions $f_{\kappa,m}$ yield the angular spectra of the internal solutions of Helmoltz equations since

$$\psi_{\kappa,m}(\mathbf{r}) \equiv \int_{\mathbb{S}_2^{(\mathbf{k})}} e^{i(\omega/c)(\hat{\mathbf{k}}\cdot\mathbf{r})}f_{\kappa,m}(\theta_k,\varphi_k)d\Omega_k \tag{28}$$

$$= a_{\kappa,m}e^{im\varphi}V_{\kappa,|m|}(\bar{\zeta})V_{-\kappa,|m|}(\bar{\eta}) \tag{29}$$

with

$$a_{\kappa,m} = (i)^{|m|}\frac{\Gamma\left(\frac{|m|+1}{2}+i\kappa\right)\Gamma\left(\frac{|m|+1}{2}-i\kappa\right)}{\Gamma^2(|m|+1)}, \tag{30}$$

and $\mathbb{S}_2^{(\mathbf{k})}$ the surface of a sphere of radius c/ω in the $\mathbf{k}$ space. The evaluation of $a_{\kappa,m}$ takes into account the integral expression for Bessel functions [17],

$$\begin{aligned}
&\int_0^\pi e^{p\cos x}[\tan(x/2)]^{2\nu}J_{2\mu}(c\sin x)dx\\
&\quad= \frac{1}{c}\left[\frac{\Gamma(\mu+\nu+1/2)}{\Gamma(2\mu+1)}\right]\left[\frac{\Gamma(\mu-\nu+1/2)}{\Gamma(2\mu+1)}\right]\\
&\quad\times M_{\nu,\mu}(z_+)M_{\nu,\mu}(z_-),\\
&z_\pm = p\pm\sqrt{p^2-c^2},
\end{aligned} \tag{31}$$

in terms of the Whittaker functions, $M_{i\kappa,\mu}(-i\eta) = \pm ie^{\pm\mu\pi i}M_{-i\kappa,\mu}(i\eta)$; here, use was made of the equation [18]

$$z^{-1/2-\mu}M_{\lambda,\mu}(z) = (-z)^{-1/2-\mu}M_{-\lambda,\mu}(-z).$$

Equations (28) and (30) guarantee

$$\int_{\mathbb{R}^3}\psi^*_{\kappa',m'}(\mathbf{r})\psi_{\kappa,m}(\mathbf{r})d^3\mathbf{r} = \delta(2\kappa-2\kappa')\delta_{m,m'}. \tag{32}$$

III. ELECTRIC AND MAGNETIC FIELDS FOR SYSTEMS WITH PARABOLIC SYMMETRY

Let us consider the vector Hertz potential [19]

$$\begin{aligned}
\mathbf{\Pi} &= \boldsymbol{\pi}e^{-i\omega t}\\
&= [\pi_1\mathbf{e}_1 + \pi_2\mathbf{e}_2 + \pi_3\mathbf{e}_3]e^{-i\omega t},
\end{aligned} \tag{33}$$

with harmonic time dependence, and Cartesian components $\pi_{1,2,3}$ that are interior solutions of the wave equation

$$\nabla^2\pi_i = -(\omega/c)^2\pi_i, \quad i = 1,2,3.$$

The frequency determines the natural unit of time $[\omega^{-1}]$ and the natural unit of length $[c/\omega]$.

The transverse character of the electromagnetic field in the absence of charge sources ($\boldsymbol{\nabla}\cdot\mathbf{E}=0=\boldsymbol{\nabla}\cdot\mathbf{B}$) as well as the Faraday law $[\boldsymbol{\nabla}\times\mathbf{E}=i(\omega/c)\mathbf{B}]$ and the Maxwell displacement equation $[\boldsymbol{\nabla}\times\mathbf{B}=-i(\omega/c)\mathbf{E}]$ are satisfied if either

$$\mathbf{E}_{\mathcal{E}}=\boldsymbol{\nabla}\times\boldsymbol{\pi}, \tag{34}$$

$$\mathbf{B}_{\mathcal{E}}=-i\frac{c}{\omega}\boldsymbol{\nabla}\times\mathbf{E}_{\mathcal{E}}, \tag{35}$$

or

$$\mathbf{B}_{\mathcal{B}}=\boldsymbol{\nabla}\times\boldsymbol{\pi}, \tag{36}$$

$$\mathbf{E}_{\mathcal{B}}=i\frac{c}{\omega}\boldsymbol{\nabla}\times\mathbf{B}_{\mathcal{B}}. \tag{37}$$

The modes given by Eqs. (34) and (35) will be referred as $\mathcal{E}$ modes, and those obtained from Eqs. (36) and (37) as $\mathcal{B}$ modes.

A. Symmetrized elementary electromagnetic modes

Elementary modes are solutions of the electromagnetic wave equations satisfying the boundary conditions derived from the physical situation under consideration, and characterized by a minimal set of elements of the labels that determine the associated vector Hertz potentials $\boldsymbol{\Pi}$. For the geometry under consideration, the most general expression of the components of $\boldsymbol{\Pi}$ are linear superpositions of solutions of the wave equation with labels $\{\omega,m,\kappa\}$. Here we show that the symmetries exhibited by the wave equation in parabolic coordinates can be used to define these elementary em modes in the presence of boundaries with parabolic geometry. The key point to define these modes corresponds to finding vector Hertz potentials which give rise to electric and magnetic fields that are eigenfunctions of the generators of the transformations associated to the symmetries mentioned in Sec. II A. For em fields, these generators take into account the expected vector behavior of $\mathbf{E}$ and $\mathbf{B}$.

Consider first an infinitesimal rotation by an angle $\delta\varphi$ about any one of the Cartesian axes. A vector field with components ϕ_r is transformed under an infinitesimal rotation by an angle $\delta\varphi$ according to the equation [20]

$$\phi_r'=\phi_r+\delta\varphi\sum_{s=1,2,3}\widehat{M}_{rsij}\phi_s, \tag{38}$$

$$=\phi_r+\delta\varphi\left[\widehat{L}_{ij}\phi_r+\sum_{s=1,2,3}\widehat{\mathcal{S}}_{rsij}\phi_s\right], \tag{39}$$

$$\widehat{L}_{ij}=-i(x_i\partial_j-x_j\partial_i), \tag{40}$$

$$\widehat{\mathcal{S}}_{rsij}=-i[\delta_{ri}\delta_{sj}-\delta_{ri}\delta_{sj}], \tag{41}$$

where the indices i,j are determined using the Levi-Civita tensor ε_{tij} for rotations about the t axis. Here, $\hat{L}_{ij}$ is the orbital angular momentum tensor operator and $\hat{\mathcal{S}}_{rsij}$ is the spin-1 tensor operator. That is, for vector fields orbital and intrinsic factors must be incorporated in their transformation.

In the case of parabolic geometry—as mentioned above for a scalar field—the symmetries are generated by rotations about the x_3 axis, and by the operator that results from the subtraction of the symmetrized product of the generator of rotations along the x_1 axis and translations along the x_2 axis, and the symmetrized product of the the generator of rotations along the x_2 axis and the translations along the x_1 axis. The operators generating these symmetries are

$$\hat{J}_3\phi_r=-i(x_1\partial_2-x_2\partial_1)\phi_r+\sum_{s=1,2,3}\widehat{\mathcal{S}}_{rs12}\phi_s, \tag{42}$$

$$\hat{\mathfrak{A}}_3\phi_r=\tfrac{1}{2}[\{\widehat{M}_{rs23},\widehat{P}_2\}-\{\widehat{M}_{rs31},\widehat{P}_1\}]\phi_s. \tag{43}$$

The symmetrized electromagnetic modes we are looking for correspond to electric $\mathbf{E}_{j,\alpha}$ and magnetic $\mathbf{B}_{j,\alpha}$ fields which satisfy Maxwell equations and are eigenvectors of the operators $\hat{J}_3$ and $\hat{\mathfrak{A}}_3$,

$$\hat{J}_3\mathbf{E}_{j,\alpha}=j\mathbf{E}_{j,\alpha},\quad \hat{J}_3\mathbf{B}_{j,\alpha}=j\mathbf{B}_{j,\alpha}, \tag{44}$$

$$\hat{\mathfrak{A}}_3\mathbf{E}_{j,\alpha}=\alpha\mathbf{E}_{j,\alpha},\quad \hat{\mathfrak{A}}_3\mathbf{B}_{j,\alpha}=\alpha\mathbf{B}_{j,\alpha}. \tag{45}$$

The coupling between the orbital and intrinsic angular momenta of the em field can be easily implemented using the circular basis

$$\mathbf{e}_{\pm}\equiv\mathbf{e}_1\pm i\mathbf{e}_2,\quad \mathbf{e}_0\equiv\mathbf{e}_3, \tag{46}$$

to write the vector Hertz potential

$$\boldsymbol{\pi}^{(m)}=\pi_+^{(m)}\mathbf{e}_+ +\pi_-^{(m)}\mathbf{e}_- +\pi_0^{(m)}\mathbf{e}_0; \tag{47a}$$

$$\pi_+^{(m)}=\sum_{\kappa}c_{\kappa,m}^{(+)}e^{i(m-1)\varphi}V_{\kappa,m-1}(\bar{\xi})V_{-\kappa,m-1}(\bar{\eta}), \tag{47b}$$

$$\pi_-^{(m)}=\sum_{\kappa}c_{\kappa,m}^{(-)}e^{i(m+1)\varphi}V_{\kappa,m+1}(\bar{\xi})V_{-\kappa,m+1}(\bar{\eta}), \tag{47c}$$

$$\pi_0^{(m)}=\sum_{\kappa}c_{\kappa,m}^{(0)}e^{im\varphi}V_{\kappa,m}(\bar{\xi})V_{-\kappa,m}(\bar{\eta}). \tag{47d}$$

Note that we have chosen to work with circular basis vectors normalized according to $\mathbf{e}_{\pm}\cdot\mathbf{e}_{\mp}=2$. By directly applying the $\hat{J}_3$ operator, it results that

$$\hat{J}_3\boldsymbol{\pi}^{(m)}=m\boldsymbol{\pi}^{(m)}, \tag{48}$$

with an analogous equation for the derived electric and magnetic fields,

$$\hat{J}_3\mathbf{E}_m=m\mathbf{E}_m,\quad \hat{J}_3\mathbf{B}_m=m\mathbf{B}_m. \tag{49}$$

In search of an adequate structure of the vector Hertz potential that also yields em fields satisfying Eq. (45) with a finite number of terms in Eqs. (47) it is necessary to work out the curl of $\boldsymbol{\pi}^{(m)}$. Written in terms of the parabolic unit vectors and scale factors,

$$\boldsymbol{\pi}^{(m)}=\left[\frac{P_+^{(m)}}{h_\eta}+\frac{\pi_0^{(m)}}{2h_\zeta}\right]\mathbf{e}_\zeta+\left[\frac{P_+^{(m)}}{h_\zeta}-\frac{\pi_0^{(m)}}{2h_\eta}\right]\mathbf{e}_\eta-iP_-^{(m)}\mathbf{e}_\varphi, \tag{50}$$

where

$$P_+^{(m)}=\frac{e^{i\varphi}\pi_+^{(m)}+e^{-i\varphi}\pi_-^{(m)}}{2},\quad P_-^{(m)}=e^{i\varphi}\pi_+^{(m)}-e^{-i\varphi}\pi_-^{(m)}. \tag{51}$$

From these equations

$$\nabla \times \boldsymbol{\pi}^{(m)} = \frac{p_\zeta^{(m)}}{h_\eta h_\varphi}\mathbf{e}_\zeta + \frac{p_\eta^{(m)}}{h_\zeta h_\varphi}\mathbf{e}_\eta + \frac{p_\varphi^{(m)}}{h_\eta h_\zeta}\mathbf{e}_\varphi,$$

$$\nabla \times (\nabla \times \boldsymbol{\pi}^{(m)}) = \frac{\mathbf{e}_\zeta}{h_\eta h_\varphi}\left[\frac{\partial}{\partial\eta}\left[\frac{h_\varphi}{h_\eta h_\zeta}p_\varphi^{(m)}\right] - im\frac{h_\eta}{h_\zeta h_\varphi}p_\eta^{(m)}\right] + \frac{\mathbf{e}_\eta}{h_\zeta h_\varphi}\left[\frac{\partial}{\partial\zeta}\left[-\frac{h_\varphi}{h_\eta h_\zeta}p_\varphi^{(m)}\right] + im\frac{h_\zeta}{h_\eta h_\varphi}p_\zeta^{(m)}\right]$$
$$+ \frac{\mathbf{e}_\varphi}{h_\zeta h_\eta}\left[\frac{\partial}{\partial\zeta}\left[-\frac{h_\eta}{h_\zeta h_\varphi}p_\eta^{(m)}\right] - \frac{\partial}{\partial\eta}\left[-\frac{h_\zeta}{h_\eta h_\varphi}p_\zeta^{(m)}\right]\right], \tag{52}$$

with

$$p_\zeta^{(m)} = i\frac{\partial h_\varphi P_-^{(m)}}{\partial\eta} - im\left[\frac{h_\eta}{h_\zeta}P_+^{(m)} - \frac{\pi_0^{(m)}}{2}\right],$$
$$p_\eta^{(m)} = -i\frac{\partial h_\varphi P_-^{(m)}}{\partial\zeta} + im\left[\frac{h_\zeta}{h_\eta}P_+^{(m)} + \frac{\pi_0^{(m)}}{2}\right], \tag{53}$$
$$p_\varphi^{(m)} = \frac{\partial}{\partial\zeta}\left[\frac{h_\eta}{h_\zeta}P_+^{(m)} - \frac{\pi_0^{(m)}}{2}\right] - \frac{\partial}{\partial\eta}\left[\frac{h_\zeta}{h_\eta}P_+^{(m)} + \frac{\pi_0^{(m)}}{2}\right].$$

In the expressions for $p_{\zeta,\eta,\varphi}^{(m)}$ we observe the presence of the differential operators

$$\hat{\mathcal{O}}_\pm^z \equiv \partial_z\sqrt{z} \pm \frac{m}{2\sqrt{z}}, \quad z = \bar{\eta}, \bar{\zeta}, \tag{54}$$

acting on the functions $V_{\kappa,m}(z)$ contained in Eqs. (47). Also in these expressions the product of $V_{\kappa,m}(z)$ by $\sqrt{z}$ is frequently found. As a consequence of this and looking at Eqs. (12)–(16), the functions $V_{\kappa\pm i/2}(z)$ are expected to appear in the expressions of the em fields obtained from $\boldsymbol{\pi}^{(m)}$; we then make the following compact ansatz for the vector Hertz potentials:

$$\pi_+^{(m;\kappa)} = c_{\kappa,m}^{(+)}e^{i(m-1)\varphi}V_{\kappa,m-1}(\bar{\zeta})V_{-\kappa,m-1}(\bar{\eta}), \tag{55a}$$
$$\pi_-^{(m;\kappa)} = c_{\kappa,m}^{(-)}e^{i(m+1)\varphi}V_{\kappa,m+1}(\bar{\zeta})V_{-\kappa,m+1}(\bar{\eta}), \tag{55b}$$
$$\pi_0^{(m;\kappa)} = c_{\kappa+i/2,m}^{(0)}e^{im\varphi}V_{\kappa+i/2,m}(\bar{\zeta})V_{-(\kappa+i/2),m}(\bar{\eta}) + c_{\kappa-i/2,m}^{(0)}e^{im\varphi}V_{\kappa-i/2,m}(\bar{\zeta})V_{-(\kappa-i/2),m}(\bar{\eta}), \tag{55c}$$

while looking for symmetrized elementary em modes that satisfy the eigenvalue Eq. (45). In the following paragraph the relevance of this ansatz is demonstrated.

The generator of the parabolic symmetry transformation for scalar fields was found to have a simple expression in wave-vector space, Eq. (24). Something similar occurs for the vector modes: in the wave-vector representation the generator $\hat{\mathfrak{A}}_3$ of the symmetry transformation for vector fields can be written as

$$\hat{\mathfrak{A}}_3\phi_r = i(\sin\theta_k\partial_{\theta_k} + \cos\theta_k)\phi_r - i\sum_{s=1,2,3}[(\delta_{r2}\delta_{s3} - \delta_{r3}\delta_{s2})k_2 + (\delta_{r1}\delta_{s3} - \delta_{r3}\delta_{s1})k_1]\phi_s. \tag{56}$$

In the wave-vector space,

$$\tilde{\boldsymbol{\pi}}^{(m;\kappa)} = \tilde{\pi}_+^{(m;\kappa)}\mathbf{e}_+ + \tilde{\pi}_-^{(m;\kappa)}\mathbf{e}_- + \tilde{\pi}_0^{(m;\kappa)}\mathbf{e}_0, \tag{57a}$$
$$\tilde{\pi}_+^{(m;\kappa)} = \tilde{c}_{\kappa,m}^{(+)}f_{\kappa,m-1}, \tag{57b}$$
$$\tilde{\pi}_-^{(m;\kappa)} = \tilde{c}_{\kappa,m}^{(-)}f_{\kappa,m+1}, \tag{57c}$$
$$\tilde{\pi}_0^{(m;\kappa)} = \tilde{c}_{\kappa+i/2,m}^{(0)}f_{\kappa+i/2,m} + \tilde{c}_{\kappa-i/2,m}^{(0)}f_{\kappa-i/2,m}, \tag{57d}$$

with $f_{\kappa,m}(\theta_k,\varphi_k)$ given by Eq. (26).

Define the vector

$$\tilde{\mathbf{A}}^{(\mathcal{E})} \equiv i\boldsymbol{k}\times\boldsymbol{\pi}^{(\tilde{m};\kappa)} = \tilde{A}_+^{(\mathcal{E})}\mathbf{e}_+ + \tilde{A}_-^{(\mathcal{E})}\mathbf{e}_- + \tilde{A}_3^{(\mathcal{E})}\mathbf{e}_3, \tag{58a}$$
$$\tilde{A}_\pm^{(\mathcal{E})} = \tfrac{1}{2}\left[\tilde{A}_1^{(\mathcal{E})} \mp i\tilde{A}_2^{(\mathcal{E})}\right] = \tfrac{1}{2}[\mp\sin\theta_k e^{\mp i\varphi}\tilde{\pi}_0^{(m;\kappa)} \pm 2\cos\theta_k\tilde{\pi}_\pm^{(m;\kappa)}], \tag{58b}$$
$$\tilde{A}_3^{(\mathcal{E})} = -\sin\theta_k[e^{i\varphi}\tilde{\pi}_+^{(m;\kappa)} - e^{-i\varphi}\tilde{\pi}_-^{(m;\kappa)}], \tag{58c}$$

proportional to the electric (magnetic) field of the $\mathcal{E}$ mode ($\mathcal{B}$ mode) in this space. Using trigonometric identities it can be shown that

$$\sin\theta_k\tan(\theta_k/2) = 1 - \cos\theta_k,$$
$$\sin\theta_k[\tan(\theta_k/2)]^{-1} = 1 + \cos\theta_k, \tag{59}$$

and $\tilde{\mathbf{A}}^{(\mathcal{E})}$ is found to be an analytic function of θ_k. For $\tilde{\mathbf{A}}^{(\mathcal{E})}$ to be an eigenvector of $\hat{\mathfrak{A}}_3$ with eigenvalue $\alpha = 2\kappa$, the coefficients $\{\tilde{c}_{\kappa,m}\}$ must satisfy the equation

$$\tilde{c}_{\kappa,m}^{(+)} + \tilde{c}_{\kappa,m}^{(-)} + \tilde{c}_{\kappa+i/2,m}^{(0)} - \tilde{c}_{\kappa-i/2,m}^{(0)} = 0. \tag{60}$$

Demanding that the following vector

$$\tilde{\mathbf{A}}^{(\mathcal{B})} = -\hat{\boldsymbol{k}}\times(\hat{\boldsymbol{k}}\times\tilde{\boldsymbol{\pi}}^{(m;\kappa)}) = \tilde{A}_+^{(\mathcal{B})}\mathbf{e}_+ + \tilde{A}_-^{(\mathcal{B})}\mathbf{e}_- + \tilde{A}_3^{(\mathcal{B})}\mathbf{e}_3, \tag{61}$$

with

$$\tilde{A}_\pm^{(\mathcal{B})} = \tfrac{1}{2}[\cos^2\theta_k\tilde{\pi}_\pm^{(m;\kappa)} - \sin^2\theta_k e^{\mp i2\varphi}\tilde{\pi}_\mp^{(m;\kappa)} - \sin\theta_k\cos\theta_k\tilde{\pi}_0], \tag{62a}$$
$$\tilde{A}_3^{(\mathcal{B})} = -\sin\theta_k\cos\theta_k[e^{i\varphi}\tilde{\pi}_+^{(m;\kappa)} + e^{-i\varphi}\tilde{\pi}_-^{(m;\kappa)}] + \sin^2\theta_k\tilde{\pi}_0^{(m;\kappa)}, \tag{62b}$$

to be an eigenvector of $\hat{\mathfrak{A}}_3$, leads to the same relationship, Eq. (60), for the coefficients $\{\tilde{c}_{\kappa,m}\}$.

Summarizing, the electric and magnetic fields obtained from either Eqs. (34) and (35) or Eqs. (36) and (37) are eigenvectors of the generator of $\hat{J}_3$ with eigenvalue m and the generator $\hat{\mathfrak{A}}_3$ with eigenvalue 2κ, whenever the Hertz potentials in wave-vector space, Eqs. (57), involve coefficients $\{\tilde{c}_{\kappa,m}\}$ satisfying Eq. (60). The operator $\hat{\mathfrak{A}}_3$ is Hermitian if κ is restricted to real values, in analogy to the results found for the scalar field.

B. Scalar product for the electromagnetic modes. Field quantization: photons with parabolic symmetries

The overlap of different em field modes can be estimated via a scalar product. Let us consider a pair of monochromatic

em modes with common frequency ω and properties labeled by a, b. Their scalar product is defined by

$$\langle a|b\rangle = \frac{1}{4\pi}\int_{\mathbb{R}^3} d^3x[\mathbf{E}_a^*(\mathbf{x})\cdot\mathbf{E}_b(\mathbf{x}) + \mathbf{B}_a^*(\mathbf{x})\cdot\mathbf{B}_b(\mathbf{x})]. \quad (63)$$

In the case $a = b$, the integrand corresponds to the time averaged em energy density,

$$\rho^{\text{em}}_{\text{Energy}} = \frac{1}{4\pi}[\mathbf{E}_a^*(\mathbf{x})\cdot\mathbf{E}_a(\mathbf{x}) + \mathbf{B}_a^*(\mathbf{x})\cdot\mathbf{B}_a(\mathbf{x})]. \quad (64)$$

For parabolic modes the involved integrals can be performed directly when the electric and magnetic fields are expressed in terms of their angular spectrum. The elementary modes in the presence of parabolic boundaries involve $\mathbf{E}_a$ and $\mathbf{B}_a$ with angular spectra derived from a Hertz potential

$$\boldsymbol{\pi}^{(a)} = \int d^3k\delta(|\mathbf{k}| - \omega/c)e^{i\mathbf{k}\cdot\mathbf{r}}\left[\tilde{\pi}_+^{(a)}\mathbf{e}_+ + \tilde{\pi}_-^{(a)}\mathbf{e}_- + \tilde{\pi}_0^{(a)}\mathbf{e}_0\right]$$

with the structure given by Eqs. (57a)–(57d). According to the results we have shown, the indices summarized with the label a include the frequency ω and the eigenvalues m and κ as well as the procedure by which $\mathbf{E}$ and $\mathbf{B}$ were evaluated from the Hertz potentials, Eqs. (34)–(37).

Two Hertz potentials will lead to the same em mode—up to a normalization factor—if a linear combination of them can be written as the gradient of a field. In such a case, the two Hertz potentials are said to be related by a gauge transformation. In wave vector space, the particular solution of Eq. (60),

$$\tilde{c}^{(+)}_{\kappa,m} = \tilde{c}^{(-)}_{\kappa,m} = -\tilde{c}^{(0)}_{\kappa+i/2,m} = \tilde{c}^{(0)}_{\kappa-i/2,m}, \quad (65)$$

corresponds to

$$\tilde{\boldsymbol{\pi}}_{\text{gauge}} = 2\mathbf{k}\left[\frac{e^{im\varphi_k}}{2\pi}\frac{[\tan(\theta_k/2)]^{-2\kappa i}}{\sin^2\theta_k}\right] \quad (66)$$

and satisfies $\mathbf{k}\times\tilde{\boldsymbol{\pi}}_{\text{gauge}} = 0$, so that $\tilde{\boldsymbol{\pi}}_{\text{gauge}}$ induces a gauge transformation. The scalar product Eq. (63) is gauge invariant.

A direct calculation shows that the electric fields $\mathbf{E}_{a,b}$ and the magnetic fields $\mathbf{B}_{a,b}$ contribute equally to $\langle a|b\rangle$ whenever they are obtained from vector Hertz potentials $\boldsymbol{\pi}^{(a,b)}$ through Eqs. (34) and (35) or Eqs. (36) and (37). Besides,

$$\begin{aligned}\langle a|b\rangle = (2\pi)^2\left(\frac{\omega}{c}\right)^2\delta_{m_a,m_b}\Bigg[&\delta_1^{(a:b)}\delta[2(\kappa_b-\kappa_a)]\\ &+\delta_2^{(a:b)}\frac{1}{4\sinh(\kappa_b-\kappa_a)\pi}\\ &+\delta_3^{(a:b)}\left[\delta[2(\kappa_b-\kappa_a)] - \frac{\kappa_b-\kappa_a}{\sinh(\kappa_b-\kappa_a)\pi}\right]\Bigg]\end{aligned}$$

with

$$\begin{aligned}\delta_1^{(a:b)} &= \left(\tilde{c}^{(+)*}_{\kappa_a,m} - \tilde{c}^{(-)*}_{\kappa_a,m}\right)\left(\tilde{c}^{(+)}_{\kappa_b,m} - \tilde{c}^{(-)}_{\kappa_b,m}\right)\\ &\quad+\left(\tilde{c}^{(0)*}_{\kappa_a+i/2,m} + \tilde{c}^{(0)*}_{\kappa_a-i/2,m}\right)\left(\tilde{c}^{(0)}_{\kappa_b+i/2,m} + \tilde{c}^{(0)}_{\kappa_b-i/2,m}\right),\\ \delta_2^{(a:b)} &= \left(\tilde{c}^{(+)*}_{\kappa_a,m} + \tilde{c}^{(-)*}_{\kappa_a,m} + \tilde{c}^{(0)*}_{\kappa_a+i/2,m} - \tilde{c}^{(0)*}_{\kappa_a-i/2,m}\right)\\ &\quad\times\left(\tilde{c}^{(+)}_{\kappa_b,m} + \tilde{c}^{-}_{\kappa_b,m} + \tilde{c}^{0}_{\kappa_b+i/2,m} - \tilde{c}^{(0)}_{\kappa_b-i/2,m}\right),\end{aligned}$$

$$\begin{aligned}\delta_3^{(a:b)} &= 2\left(\tilde{c}^{(0)*}_{\kappa_a+i/2,m}\tilde{c}^{(0)}_{\kappa_b+i/2,m} - \tilde{c}^{(0)*}_{\kappa_a-i/2,m}\tilde{c}^{(0)}_{\kappa_b-i/2,m}\right)\\ &\quad-\left(\tilde{c}^{(+)*}_{\kappa_a,m} + \tilde{c}^{(-)*}_{\kappa_a,m}\right)\left(c^{(0)}_{\kappa_b+i/2,m} + c^{(0)}_{\kappa_b-i/2,m}\right)\\ &\quad-\left(\tilde{c}^{(+)}_{\kappa_b,m} + \tilde{c}^{(-)}_{\kappa_b,m}\right)\left(c^{(0)*}_{\kappa_a+i/2,m} + c^{(0)*}_{\kappa_a-i/2,m}\right). \quad (67)\end{aligned}$$

Notice that Eq. (60) guarantees that for symmetrized elementary modes $\delta_2^{(a:b)} = 0 = \delta_3^{(a:b)}$, thus implying the orthogonality between modes with different m or κ.

By demanding

$$\left(\frac{2\pi\omega}{c}\right)^2\delta_1^{(a:b)} = \hbar\omega, \quad (68)$$

the symmetrized modes can be used to define the electric-field operator

$$\hat{\mathbf{E}}(\mathbf{x},t) = \int d\omega\sum_a(\mathbf{E}_a(\mathbf{x})e^{-i\omega t}\hat{\mathrm{a}}_{a,\omega} + \mathbf{E}_a^*(\mathbf{x})e^{i\omega t}\hat{\mathrm{a}}^\dagger_{a,\omega}) \quad (69)$$

and the magnetic field operator

$$\hat{\mathbf{B}}(\mathbf{x},t) = \int d\omega\sum_a(\mathbf{B}_a(\mathbf{x})e^{-i\omega t}\hat{\mathrm{a}}_{a,\omega} + \mathbf{B}_a^*(\mathbf{x})e^{i\omega t}\hat{\mathrm{a}}^\dagger_{a,\omega}) \quad (70)$$

by introducing the creation and annihilation operators

$$[\hat{\mathrm{a}}_{a,\omega}, \hat{\mathrm{a}}^\dagger_{a',\omega'}] = \delta_{a,a'}\delta(\omega-\omega'). \quad (71)$$

The dynamical variables of the electromagnetic field define its mechanical identity. These variables can be interpreted as properties of photons via the quantization of the em field in terms of vectorial modes with the adequate space-time dependence. For Cartesian symmetry the modes are properly described by plane waves where the photon frequency ω, wave vector $\mathbf{k}$, and helicity σ (projection of the polarization vector on the wave vector) determine the photon energy, linear momentum, and intrinsic angular momentum, respectively. For optical systems displaying circular cylinder symmetry, Bessel modes are used to define photons with frequency ω, transverse wave vector component $k_\perp$, azymuthal phase quantum number m, and helicity σ, and relate them to the photon energy, transverse linear momentum, orbital, and intrinsic angular momentum respectively [21]. In general, via the Noether theorem, the generator of a given symmetry of a system leads to the identification of a dynamical variable that is conserved even under interaction between subsystems. The expected expression for the density of the electromagnetic dynamical variable related to the parabolic symmetry generator $\hat{\mathfrak{A}}_3$ remains to be explored. It could be extrapolated from previous results obtained for non-Cartesian geometries such as circular [21], elliptic [22], and parabolic [23] cylinder symmetries which, contrary to parabolic symmetry, exhibit covariance under translations along the cylinder axis.

For a parabolic cylinder geometry the symmetry generators are $\hat{P}_3$ and the operator $(\hat{J}_3\hat{P}_2 + \hat{P}_2\hat{J}_3)/2$, if $\mathbf{e}_3$ defines the cylinder axis and $\mathbf{e}_2$ is parallel to the axes of symmetry of the parabolas that define the corresponding coordinate. The mechanical effects of em waves displaying parabolic cylinder geometry have been experimentally studied as reported in Ref. [24]. It was observed that coherent light in an elementary mode with such symmetry modifies the center-of-mass

motion of ultracold atoms in a way naturally described by the parabolic cylinder momentum $(j_3 p_2 + p_2 j_3)/2$ defined in terms of the total angular $\mathbf{j}$ and linear momentum $\mathbf{p}$ of each atom. In that work the transfer of that dynamical variable from light to matter was quantified; the results were compatible with a conservation law.

An analogous effect could be studied for parabolic symmetries, now concerning the $\hat{\mathfrak{A}}_3$ operator. In fact, as already mentioned, for a material particle $(1/2)(\{j_1, p_2\} - \{j_2, p_1\})$ corresponds to the kinetic part of the Runge-Lenz vector which plays an important role in the classical and quantum study of the particle mechanical response to its coupling to a central field. These ideas provide a motivation to study the mechanical properties of the em field in parabolic symmetries interacting with material particles for a better understanding of the significance of the variable $2\hbar\kappa$ which emerges as a property of photons in optical systems with parabolic symmetry. Notice that such a study could also give a different perspective on the dynamics of highly focused em waves in three dimensions interacting with matter both in the classical and quantum realms. Those waves could be generated by a parabolic mirror.

IV. VECTORIAL MODES IN THE PRESENCE OF A PARABOLIC MIRROR

The physical configuration at hand determines the natural geometry to describe the em field. In the following section, the effect of an ideal parabolic mirror over the elementary modes is studied. An ideal reflecting mirror with parabolic geometry is a paradigmatic optical system. The description of its focusing properties in terms of rays has been known for a long time. The electromagnetic system, however, admits modes with interesting nontrivial configurations both linked to the vector character of the field and the possibility of singularities in its phase.

Consider an ideal parabolic mirror located at $\zeta = \zeta_0$. Boundary conditions imply that the magnetic-field component normal to the mirror must vanish at its surface,

$$\mathbf{B} \cdot \mathbf{e}_\zeta|_{\zeta=\zeta_0} = 0, \tag{72}$$

as well as the tangential components of the electric field,

$$\mathbf{E} \cdot \mathbf{e}_\eta|_{\zeta=\zeta_0} = 0, \quad \mathbf{E} \cdot \mathbf{e}_\varphi|_{\zeta=\zeta_0} = 0. \tag{73}$$

The general form of any em wave in the presence of the parabolic mirror can be written as a linear combination of both the modes $\{\mathbf{E}_\mathcal{E}, \mathbf{B}_\mathcal{E}\}$ and $\{\mathbf{E}_\mathcal{B}, \mathbf{B}_\mathcal{B}\}$ that satisfy the conditions given by Eqs. (72) and (73). These three conditions are not independent due to Maxwell equations that relate $\mathbf{E}$ and $\mathbf{B}$. For $\mathcal{E}$ modes this can be shown by writing the em field in terms of the $p^{(m)}_{\zeta,\eta,\varphi}$ functions using Eqs. (52). A direct calculation shows that the boundary conditions are fulfilled by demanding two conditions only:

$$p^{(m)}_\eta|_{\zeta=\zeta_0} = 0, \quad p^{(m)}_\varphi|_{\zeta=\zeta_0} = 0, \tag{74}$$

for $\zeta = \zeta_0$ and any η and φ. For $\mathcal{B}$ modes the boundary conditions at the mirror surface translate to the three equations:

$$p^{(m)}_\zeta\big|_{\zeta=\zeta_0} = 0, \tag{75}$$

$$\frac{\partial}{\partial\zeta}\left[-\frac{h_\varphi}{h_\eta h_\zeta} p^{(m)}_\varphi\right] + im\frac{h_\zeta}{h_\eta h_\varphi} p^{(m)}_\zeta\bigg|_{\zeta=\zeta_0} = 0, \tag{76}$$

$$\frac{\partial}{\partial\zeta}\left[-\frac{h_\eta}{h_\zeta h_\varphi} p^{(m)}_\eta\right] - \frac{\partial}{\partial\eta}\left[-\frac{h_\zeta}{h_\eta h_\varphi} p^{(m)}_\zeta\right]\bigg|_{\zeta=\zeta_0} = 0. \tag{77}$$

To show that Eqs. (75)–(77) are not independent and can reduce to only two conditions is not as direct as for $\mathcal{E}$ modes. However, the following general argument can be used. Since for any well behaved vector Hertz potential $\boldsymbol{\pi}$

$$\boldsymbol{\nabla} \times (\boldsymbol{\nabla} \times \boldsymbol{\pi}) = \boldsymbol{\nabla}(\boldsymbol{\nabla} \cdot \boldsymbol{\pi}) - \nabla^2\boldsymbol{\pi} = \boldsymbol{\nabla}(\boldsymbol{\nabla} \cdot \boldsymbol{\pi}) + (\omega/c)^2\boldsymbol{\pi},$$

demanding

$$\mathbf{e}_\zeta \times (\boldsymbol{\nabla} \times (\boldsymbol{\nabla} \times \boldsymbol{\pi}))|_{\zeta=\zeta_0} = 0 \tag{78}$$

for $\zeta = \zeta_0$ and any value of η and φ, guarantees that the tangential derivatives of these quantities are also zero at $\zeta = \zeta_0$, and as a consequence

$$\mathbf{e}_\zeta \cdot \boldsymbol{\nabla} \times \boldsymbol{\pi}|_{\zeta=\zeta_0} = (c/\omega)^2\{\mathbf{e}_\zeta \cdot \boldsymbol{\nabla} \times [\boldsymbol{\nabla} \times (\boldsymbol{\nabla} \times \boldsymbol{\pi}) - \boldsymbol{\nabla}(\boldsymbol{\nabla} \cdot \boldsymbol{\pi})]\}|_{\zeta=\zeta_0} = 0.$$

Equation (78) can be expressed in terms of $P^{(m)}_\pm$ and $\pi^{(m)}_0$ for the $\boldsymbol{\pi}^{(m)}$ vector Hertz potentials. The resulting pair of equations seems to be difficult to solve until it is noticed that (i) they must be satisfied simultaneously for $\zeta = \zeta_0$ and any value of φ and η, and (ii) $\sqrt{\eta}V_{-\kappa,m}(\eta)$ satisfies the Whittaker equation. These facts lead to the simplified equations

$$\left[\frac{\partial\sqrt{\bar\zeta\bar\eta}P^{(m)}_-}{\partial\bar\eta} - \frac{m}{\bar\eta}\sqrt{\bar\zeta\bar\eta}P^{(m)}_+ + m\frac{\pi^{(m)}_0}{2}\right]\bigg|_{\zeta=\zeta_0} = 0, \tag{79}$$

$$\left[\frac{\partial\sqrt{\bar\zeta\bar\eta}P^{(m)}_+}{\partial\bar\zeta} + \bar\zeta\frac{\partial\pi^{(m)}_0/2}{\partial\bar\zeta} - \left[\frac{\kappa}{m} + \frac{m}{4\bar\zeta} - \frac{\bar\zeta}{4m}\right]\sqrt{\bar\zeta\bar\eta}P^{(m)}_-\right]\bigg|_{\zeta=\zeta_0} = 0. \tag{80}$$

A. Symmetrized modes in the presence of mirrors

The boundary conditions imposed by an ideal parabolic mirror can be studied using the Hertz potentials $\boldsymbol{\pi}^{(m)}$ given by Eq. (47) as summations over terms containing the functions $V_{\kappa,m}$. This gives rise to a hierarchy of equations described in detail in Appendix B for the $\mathcal{E}$ modes. Two different scenarios are identified. The first corresponds to modes with a null eigenvalue of $\hat{J}_3$. In such a case, the indices of the functions $V_{\kappa,m}$ in the Hertz potentials are just $m = 0, 1$. The second scenario corresponds to a nonzero eigenvalue of $\hat{J}_3$. Then, the relevant m values in the $V_{\kappa,m}$ are 3, $|m-1|$, $|m+1|$, and $|m|$. The complexity of the equations for the coefficients of the $V_{\kappa,m}$ functions illustrates the consequences of working with modes that are only partially symmetrized when ignoring the relevance of the symmetry generated by the operator $\hat{\mathfrak{A}}_3$.

In the following paragraphs we derive the closed expressions of the *fully* symmetrized elementary modes in the presence of an ideal parabolic mirror. The corresponding $\{\mathbf{E}_\mathcal{E}, \mathbf{B}_\mathcal{E}\}$ and $\{\mathbf{E}_\mathcal{B}, \mathbf{B}_\mathcal{B}\}$ modes are obtained from the vector Hertz potentials $\pi^{(m;\kappa)}$ with components given by Eqs. (55a)–(55c). In

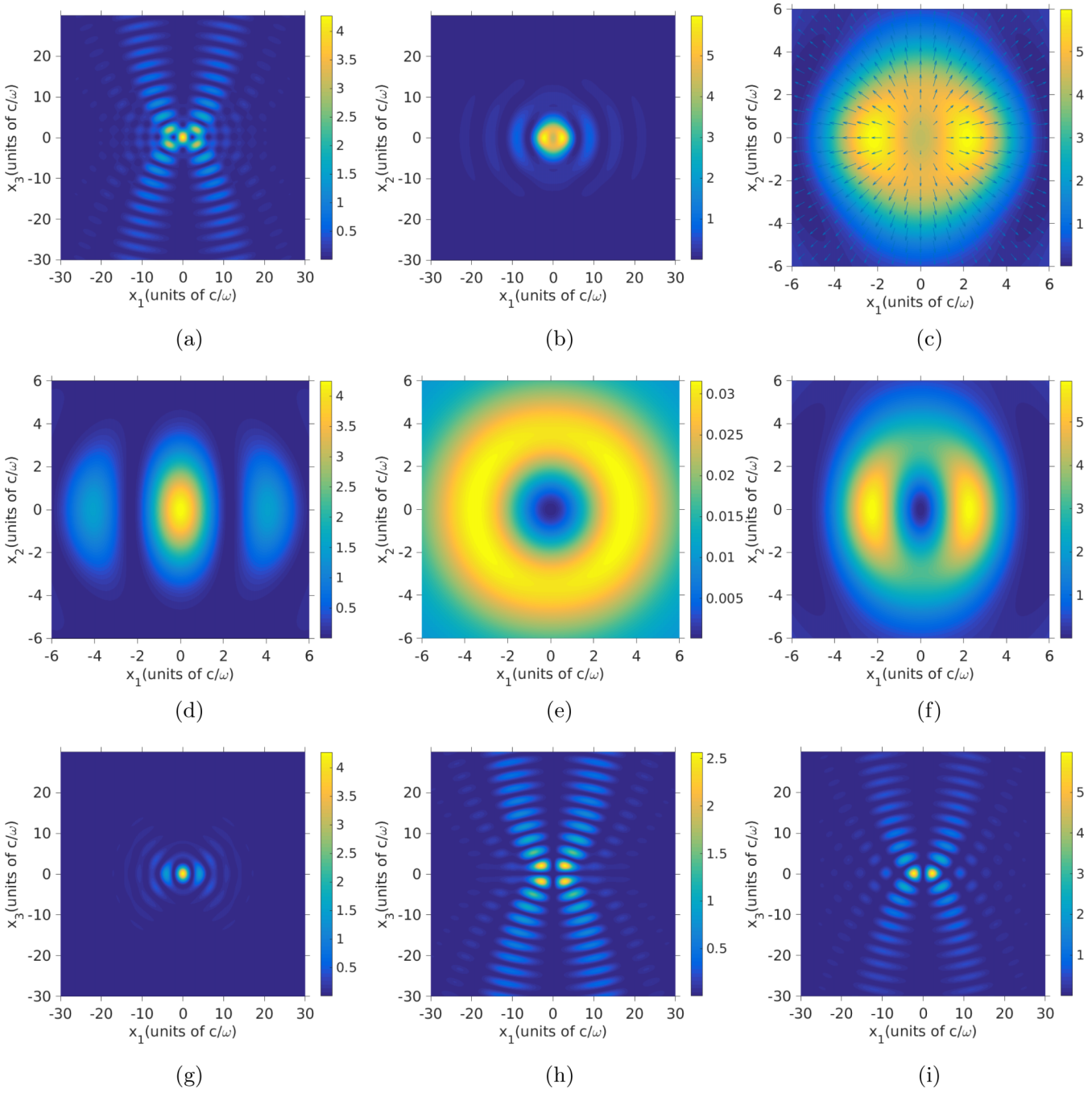

FIG. 2. Neuman mode with parameter $\kappa = -0.040\,937$ and coefficient $\tilde{c}_0 = 1$. This κ is the root with the smallest absolute value of the Neuman boundary condition, Eq. (85), for a mirror surface at $\zeta_0 = 35\,700c/\omega$. (a),(b) Illustrative example of the em energy density at the planes defined by (a) $x_1 = 0$ and (b) $x_3 = 0$. (c) Projection of the real part of the electric field into the plane $x_3 = 0$. (d)–(f) Components of the em field at the $x_3 = 0$ plane: (d) $|\mathbf{E} \times \mathbf{e}_3|^2$, (e) cylindrical radial component $|B_\rho|^2$, and (f) $|\mathbf{B} \cdot \mathbf{e}_3|^2$; (g)–(i) components of the em field at the $x_2 = 0$ plane: (g) $|\mathbf{E} \cdot \mathbf{e}_3|^2$, (h) $|\mathbf{E} \times \mathbf{e}_3|^2$, and (i) $|\mathbf{B}|^2$.

order to simplify the notation we drop out these superscripts in the expressions involving $\boldsymbol{\pi}$ from now on unless necessary.

1. Parabolic Neuman $m = 0$ em modes

For $m = 0$ we show here that the $\mathcal{E}$ modes can be derived from a simple vector Hertz potential,

$$\boldsymbol{\pi}_{m=0} = c_0[e^{-i\varphi}\mathbf{e}_+ - e^{i\varphi}\mathbf{e}_-]V_{\kappa_0,1}(\bar{\zeta})V_{-\kappa_0,1}(\bar{\eta}), \tag{81}$$

with coefficients $c^{(0)}_{\kappa\pm i/2,0} = 0$ and $c^{(+)}_{\kappa,0} = -c^{(-)}_{\kappa,0} = c_0$ satisfying Eq. (60). As a consequence, $\boldsymbol{\pi}_{m=0}$ yields em fields that are eigenfunctions of the symmetry generators $\hat{J}_3$ and $\hat{\mathfrak{A}}_3$.

The explicit expression for the electric field is

$$\mathbf{E}_N = \boldsymbol{\nabla} \times \boldsymbol{\pi}_{m=0} = 2c_0 \frac{\mathbf{e}_\zeta}{h_\eta h_\varphi}\left[\sqrt{\zeta}V_{\kappa_0,1}(\bar{\zeta})\frac{\partial}{\partial\eta}\sqrt{\eta}V_{-\kappa_0,1}(\bar{\eta})\right] - 2c_0\frac{\mathbf{e}_\eta}{h_\zeta h_\varphi}\left[\sqrt{\eta}V_{-\kappa_0,1}(\bar{\eta})\frac{\partial}{\partial\zeta}\sqrt{\zeta}V_{\kappa_0,1}(\bar{\zeta})\right], \tag{82}$$

while the accompanying magnetic field $\mathbf{B}_N$ is

$$\mathbf{B}_N = 2c_0 V_{\kappa_0,1}(\bar{\zeta}) V_{-\kappa_0,1}(\bar{\eta}) \mathbf{e}_\varphi. \tag{83}$$

Since $\mathbf{e}_\zeta$ and $\mathbf{e}_\eta$ are superpositions of the radial $\mathbf{e}_\rho = \cos\varphi \mathbf{e}_1 + \sin\varphi \mathbf{e}_2$ and $\mathbf{e}_3$ vectors, Eq. (A6) in Appendix A, the boundary condition

$$\mathbf{E}_N \cdot \mathbf{e}_\varphi|_{\zeta=\zeta_0} = 0$$

is directly satisfied. Meanwhile, the boundary condition

$$\mathbf{E}_N \cdot \mathbf{e}_\eta|_{\zeta=\zeta_0} = 0$$

is equivalent to the Neuman-like equation

$$\frac{\partial}{\partial \bar{\zeta}} \sqrt{\bar{\zeta}} V_{\kappa_0,1} \Big|_{\zeta=\zeta_0} = 0. \tag{84}$$

Using Eqs. (12)–(16), it can be shown that this equation can also be written as

$$\mathcal{W}_{\kappa,0}(\bar{\zeta}_0) \equiv \frac{V_{\kappa+i/2,0}(\bar{\zeta}_0)}{V_{\kappa-i/2,0}(\bar{\zeta}_0)} = -1. \tag{85}$$

Parabolic Neuman modes were already studied in Refs. [1,2]. The $\kappa = 0$ mode yields an electric field that resembles that produced by an electric dipole.

In Fig. 2 we illustrate the properties of Neuman modes with small values of κ. The em field is highly focused. Notice that the contribution of the electric and magnetic field to the em energy density, Eq. (64), is not balanced between those fields; that is, contrary to a plane wave, $|\mathbf{E}(\mathbf{r}, t)|$ may be different to $|\mathbf{B}(\mathbf{r}, t)|$. An optical vortex is located at the origin for the radial component of the electric field, and a high similarity to a radial doughnut mode [25] near the focus of the mirror can also be observed.

2. *Parabolic Dirichlet $m = 0$ em modes*

Consider now the $\mathcal{B}$ mode derived from the vector Hertz potential given in Eq. (81). The resulting electric field

$$\mathbf{E}_D = \boldsymbol{\nabla} \times (\boldsymbol{\nabla} \times \boldsymbol{\pi}_{m=0})$$

has the explicit form

$$\mathbf{E}_D = -2c_0 V_{\kappa_0,1}(\bar{\zeta}) V_{-\kappa_0,1}(\bar{\eta}) \mathbf{e}_\varphi$$

so that

$$\mathbf{E}_D \cdot \mathbf{e}_\eta = 0.$$

In order for the field to satisfy

$$\mathbf{E}_D \cdot \mathbf{e}_\varphi|_{\zeta=\zeta_0} = 0,$$

the Dirichlet condition

$$V_{\kappa_0,1}(\bar{\zeta}_0) = 0 \tag{86}$$

is necessary. Equation (86) is equivalent to

$$\mathcal{W}_{\kappa,0}(\bar{\zeta}_0) \equiv \frac{V_{\kappa+i/2,0}(\bar{\zeta}_0)}{V_{\kappa-i/2,0}(\bar{\zeta}_0)} = 1. \tag{87}$$

The polarization of the Dirichlet modes is orthogonal to that of the Neuman modes.

In Fig. 3 the Dirichlet modes with small value of $|\kappa|$ are illustrated. We have chosen the same location of the parabolic mirror as the one used in Fig. 2. Though the values of κ for the illustrated Neuman and Dirichlet modes are similar, their general structure and configurations for their $\mathbf{E}$ and $\mathbf{B}$ fields are very different near the focus.

3. *$\{\mathbf{E}_\mathcal{B}, \mathbf{B}_\mathcal{B}\}$ symmetrized elementary modes for $m > 0$*

We now consider the general structure of the vector Hertz potential, given by Eqs. (55a)–(55c) in configuration space and by Eqs. (57a)–(57d) in wave-vector space, to construct the elementary $\mathcal{B}$ modes for $m > 0$. The boundary conditions for $\mathcal{B}$ modes, Eqs. (79) and (80), are equivalent to a set of linear equations for the coefficients $\{\tilde{c}^{(\pm)}_{\kappa,m}, \tilde{c}^{(0)}_{\kappa\pm i/2,m}\}_\mathcal{B}$; in matricial form these equations are

$$\mathbb{M}_\mathcal{B}\mathbb{C}_\mathcal{B} =: \begin{pmatrix} d_+ + d_-\mathcal{W}_{\kappa,m} & \mathcal{W}_{\kappa,m} - 1 & -\mathcal{W}_{\kappa,m} & 0 \\ 1 & \mathcal{W}_{\kappa,m} & -\mathcal{W}_{\kappa,m} - 1 & 0 \\ d_+ + d_-\mathcal{W}_{\kappa,m} & 1 - \mathcal{W}_{\kappa,m} & 0 & 1 \\ d_+ & -d_-\mathcal{W}_{\kappa,m} & 0 & d_+ - d_-\mathcal{W}_{\kappa,m} \end{pmatrix} \begin{pmatrix} \tilde{c}^{(+)}_{\kappa,m} \\ \tilde{c}^{(-)}_{\kappa,m} \\ \tilde{c}^{(0)}_{\kappa+i/2,m} \\ \tilde{c}^{(0)}_{\kappa-i/2,m} \end{pmatrix} = 0, \tag{88}$$

with

$$\mathcal{W}_{\kappa,m}(\bar{\zeta}_0) = \frac{V_{\kappa+i/2,m}(\bar{\zeta}_0)}{V_{\kappa-i/2,m}(\bar{\zeta}_0)}. \tag{89}$$

The existence of nontrivial solutions to this equation is conditioned to the existence of κ values for which

$$\mathrm{Det}\mathbb{M}_\mathcal{B} = \left(d_+ + d_-\mathcal{W}^2_{\kappa,m}\right)\left(d_+\mathcal{W}_{\kappa,m} - d_-\mathcal{W}^2_{\kappa,m} - d_+\right) = 0. \tag{90}$$

Since $|d_+/d_-| = 1 = |\mathcal{W}_{\kappa,m}|$, the condition

$$d_+ + d_-\mathcal{W}^2_{\kappa,m} = 0 \Rightarrow \mathcal{W}^2_{\kappa,m} = \frac{V^2_{\kappa+i/2,m}(\bar{\zeta}_0)}{V^2_{\kappa-i/2,m}(\bar{\zeta}_0)} = -\frac{d_+}{d_-} \tag{91}$$

is feasible, while the condition

$$d_+\mathcal{W}_{\kappa,m} - d_-\mathcal{W}^2_{\kappa,m} - d_+ = 0 \Rightarrow 1 = |\mathcal{W}_{\kappa,m}| = \frac{1}{2}\left|1 \pm \sqrt{1 - 4\frac{d_+}{d_-}}\right| \tag{92}$$

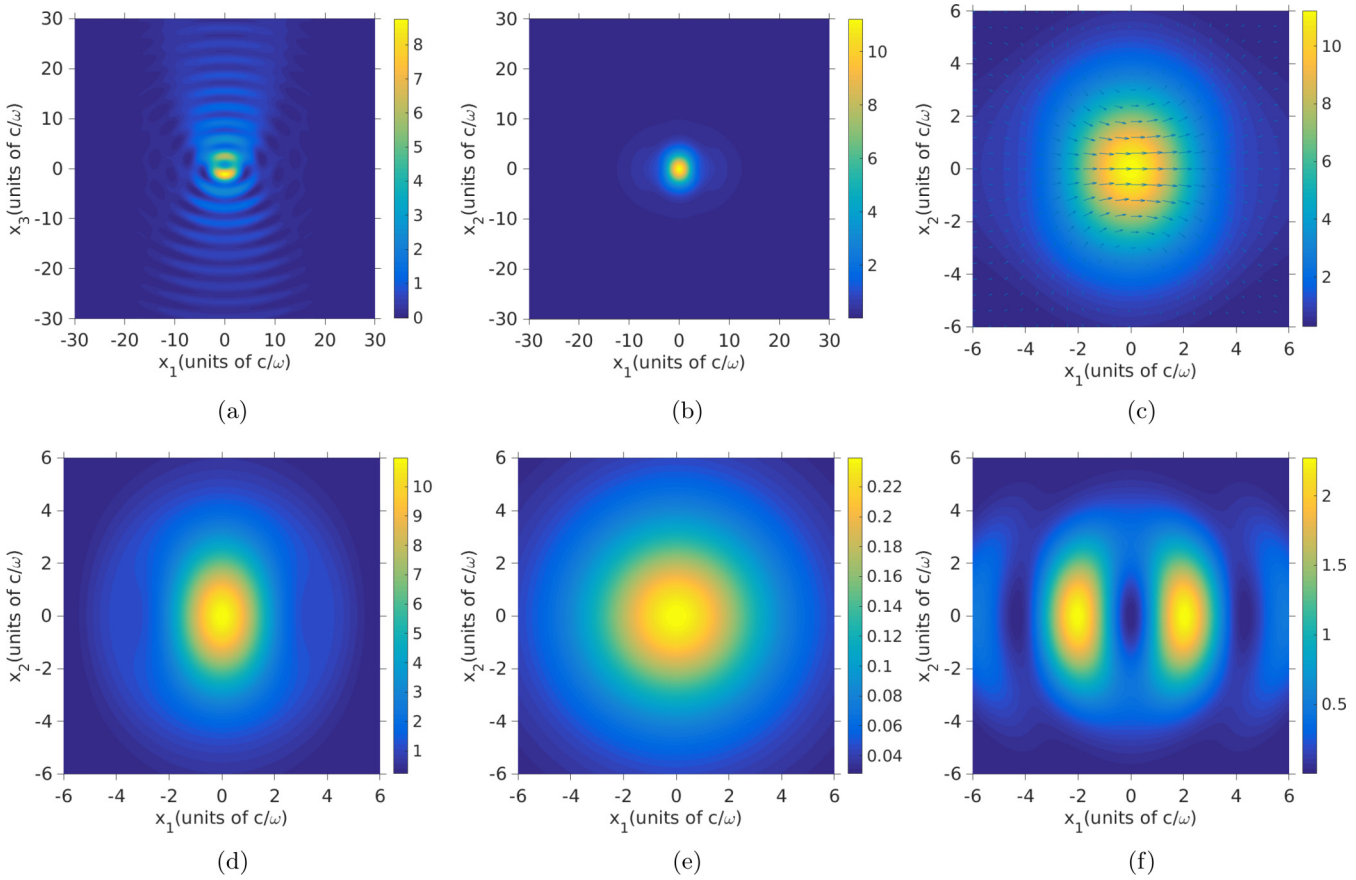

FIG. 3. Dirichlet mode with parameter $\kappa = -0.055\,760\,6$ and coefficient $\tilde{c}_0 = 1$. This κ is the root with the smallest absolute value of the Dirichlet boundary condition, Eq. (86), for a mirror surface at $\zeta_0 = 35\,700c/\omega$. (a),(b) Illustrative example of the em energy density at the planes defined by (a) $x_2 = 0$ and (b) $x_3 = 0$. (c) Electric-field projection into the plane $x_3 = 0$. (d)–(f) Components of the em field at the $x_3 = 0$ plane: (d) $|\mathbf{E} \times \mathbf{e}_3|^2$, (e) cylindrical radial component $|B_\rho|^2$, and (f) $|\mathbf{B} \cdot \mathbf{e}_3|^2$.

is not. Notice that

$$\frac{d_-}{d_+}\mathcal{W}_{\kappa,m} + \mathcal{W}^*_{\kappa,m} = 0$$
$$\Rightarrow d_- V^2_{\kappa+i/2,m}(\bar{\zeta}_0) + d_+ V^2_{\kappa-i/2,m}(\bar{\zeta}_0) = 0, \quad (93)$$

which involves, from Eq. (19), just a real valued function on the left-hand side since $V_{\kappa+i/2,m}(\bar{\zeta}_0) = V^*_{\kappa-i/2,m}(\bar{\zeta}_0)$ for real κ and ζ_0 and implies the relation $\mathcal{W}^*_{\kappa,m} = \mathcal{W}^{-1}_{\kappa,m}$.

Two sets of solutions to Eq. (88) are

$$\tilde{c}^{(+)}_{\kappa,m} = 0, \quad (94a)$$
$$\tilde{c}^{(0)}_{\kappa+i/2,m} = (1 - \mathcal{W}^*_{\kappa,m}) d_+ \tilde{c}^{(-)}_{\kappa,m}, \quad (94b)$$
$$\tilde{c}^{(0)}_{\kappa-i/2,m} = -(1 - \mathcal{W}_{\kappa,m}) d_- \tilde{c}^{(-)}_{\kappa,m}, \quad (94c)$$

and

$$\tilde{c}^{(-)}_{\kappa,m} = 0, \quad (95a)$$
$$\tilde{c}^{(0)}_{\kappa+i/2,m} = (d_+ \mathcal{W}^*_{\kappa,m} + d_-) \tilde{c}^{(+)}_{\kappa,m}, \quad (95b)$$
$$\tilde{c}^{(0)}_{\kappa-i/2,m} = -(d_- \mathcal{W}_{\kappa,m} + d_+) \tilde{c}^{(+)}_{\kappa,m}. \quad (95c)$$

We emphasize that the boundary condition given in Eq. (91) guarantees that the coefficients $\{\tilde{c}^{(\pm)}_{\kappa,m}, \tilde{c}^{(0)}_{\kappa\pm i/2,m}\}_{\mathcal{B}}$ satisfy Eq. (60) and, as a consequence, $\mathbf{E}_{\mathcal{B}}$ and $\mathbf{B}_{\mathcal{B}}$ are eigenvectors of $\hat{J}_3$ and $\hat{\mathfrak{A}}_3$. Note also that the two sets of solutions, Eqs. (94a)–(94c) and (95a)–(95c), lead to the same electromagnetic mode since a linear combination of them can be written as a gradient of a field with the form given in Eqs. (65) and (66).

The $\mathcal{B}$ modes are illustrated for small values of κ in Fig. 4. An optical vortex is observed for the x_3 component of the electric field at the XY plane. Notice that the components of the electric field exemplified in Fig. 4(c) correspond to the real part of Eq. (37), while Fig. 4(d) shows the modulus $(\mathbf{E} \times \mathbf{e}_3) \cdot (\mathbf{E}^* \times \mathbf{e}_3)$. For the illustrated $\mathcal{B}$ mode, the em energy density is of purely magnetic origin at the focus of the mirror.

4. $\{\mathbf{E}_{\mathcal{E}}, \mathbf{B}_{\mathcal{E}}\}$ *symmetrized elementary modes for* $m > 0$

The structure of a vector Hertz potential for a symmetrized em mode is the same as that used for the $\{\mathbf{E}_{\mathcal{B}}, \mathbf{B}_{\mathcal{B}}\}$ modes. The boundary conditions for $\mathcal{E}$ modes given in Eq. (74) leads to the

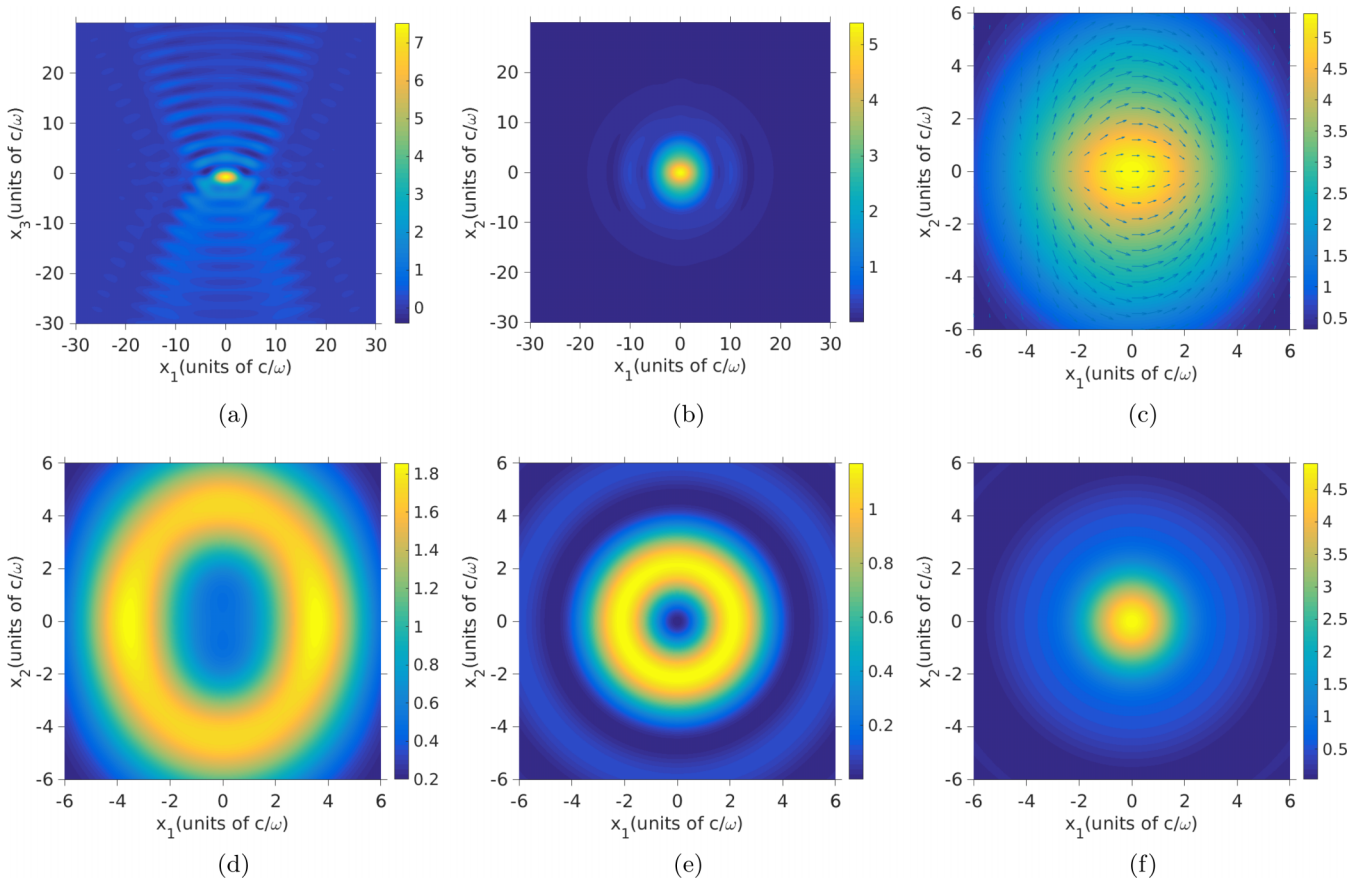

FIG. 4. $\mathcal{B}$ mode with parameters $m = 1$, $\kappa = 0.032\,372\,77$ and coefficients $c^{(+)}_{\kappa,1} = 1$, $c^{(-)}_{\kappa,1} = 0$. This κ has the smallest absolute value among the roots of the boundary condition Eq. (93) for a mirror surface at $\zeta_0 = 35\,700c/\omega$. (a),(b) Illustrative example of the em energy density at the planes defined by (a) $x_2 = 0$ and (b) $x_3 = 0$. (c) Electric-field projection into the plane $x_3 = 0$. (d)–(f) Components of the em field at the $x_3 = 0$ plane: (d) $|\mathbf{E} \times \mathbf{e}_3|^2$, (e) $|\mathbf{E} \cdot \mathbf{e}_3|^2$, and (f) $|\mathbf{B} \times \mathbf{e}_3|^2$.

matricial equation

$$\mathbb{M}_{\mathcal{E}}\mathbb{C}_{\mathcal{E}} =: \begin{pmatrix} 1 & -\mathcal{W}_{\kappa,m} & \mathcal{W}_{\kappa,m} - 1 & 0 \\ 0 & \mathcal{W}_{\kappa,m} + \frac{d_+}{d_-}\mathcal{W}^*_{\kappa,m} & -(\mathcal{W}_{\kappa,m} + \frac{d_+}{d_-}\mathcal{W}^*_{\kappa,m}) & 0 \\ 1 & -\mathcal{W}^*_{\kappa,m} & 0 & 1 - \mathcal{W}^*_{\kappa,m} \\ 0 & \mathcal{W}^*_{\kappa,m} + \frac{d_-}{d_+}\mathcal{W}_{\kappa,m} & 0 & \mathcal{W}^*_{\kappa,m} + \frac{d_-}{d_+}\mathcal{W}_{\kappa,m} \end{pmatrix} \begin{pmatrix} \tilde{c}^{(+)}_{\kappa,m} \\ \tilde{c}^{(-)}_{\kappa,m} \\ \tilde{c}^{(0)}_{\kappa+i/2,m} \\ \tilde{c}^{(0)}_{\kappa-i/2,m} \end{pmatrix} = 0, \tag{96}$$

for the $\{\tilde{c}^{(\pm)}_{\kappa,m}, \tilde{c}^{(0)}_{\kappa\pm i/2}\}_{\mathcal{E}}$ in the wave vector representation of the Hertz potential.

The consistency of these equations requires

$$\mathrm{Det}\mathbb{M}_{\mathcal{E}} = -2\left|\frac{d_-}{d_+}\mathcal{W}_{\kappa,m} + \mathcal{W}^*_{\kappa,m}\right|^2 = 0, \tag{97}$$

a condition, involving a real valued function of ζ_0, that *coincides with that for $\mathcal{B}$ modes*, Eq. (93).

Assuming the fulfillment of Eq. (97) is equivalent to just two linear equations for the four coefficients

$$\tilde{c}^{(+)}_{\kappa,m} - \mathcal{W}_{\kappa,m}\tilde{c}^{(-)}_{\kappa,m} - (1 - \mathcal{W}_{\kappa,m})\tilde{c}^{(0)}_{\kappa+i/2,m} = 0, \tag{98}$$

$$\tilde{c}^{(+)}_{\kappa,m} - \mathcal{W}^*_{\kappa,m}\tilde{c}^{(-)}_{\kappa,m} + (1 - \mathcal{W}^*_{\kappa,m})\tilde{c}^{(0)}_{\kappa-i/2,m} = 0. \tag{99}$$

A complementary condition can be taken when symmetrized $\mathcal{E}$ modes are used. This can be achieved in a similar way to the one used for $\mathcal{B}$ modes. Two sets of coefficients $\{\tilde{c}^{(\pm)}_{\kappa,m}, \tilde{c}^{(0)}_{\kappa\pm i/2,m}\}_{\mathcal{E}}$ that yield these conditions are

$$\tilde{c}^{(+)}_{\kappa,m} = 0, \tag{100a}$$

$$\tilde{c}^{(0)}_{\kappa+i/2,m} = \frac{1}{(\mathcal{W}^*_{\kappa,m} - 1)}\tilde{c}^{(-)}_{\kappa,m}, \tag{100b}$$

$$\tilde{c}^{(0)}_{\kappa-i/2,m} = -\frac{1}{(\mathcal{W}_{\kappa,m} - 1)}\tilde{c}^{(-)}_{\kappa,m}, \tag{100c}$$

and

$$\tilde{c}^{(-)}_{\kappa,m} = 0, \tag{101a}$$

$$\tilde{c}^{(0)}_{\kappa+i/2,m} = -\frac{1}{(\mathcal{W}_{\kappa,m} - 1)}\tilde{c}^{(+)}_{\kappa,m}, \tag{101b}$$

$$\tilde{c}^{(0)}_{\kappa-i/2,m} = \frac{1}{(\mathcal{W}^*_{\kappa,m} - 1)}\tilde{c}^{(+)}_{\kappa,m}. \tag{101c}$$

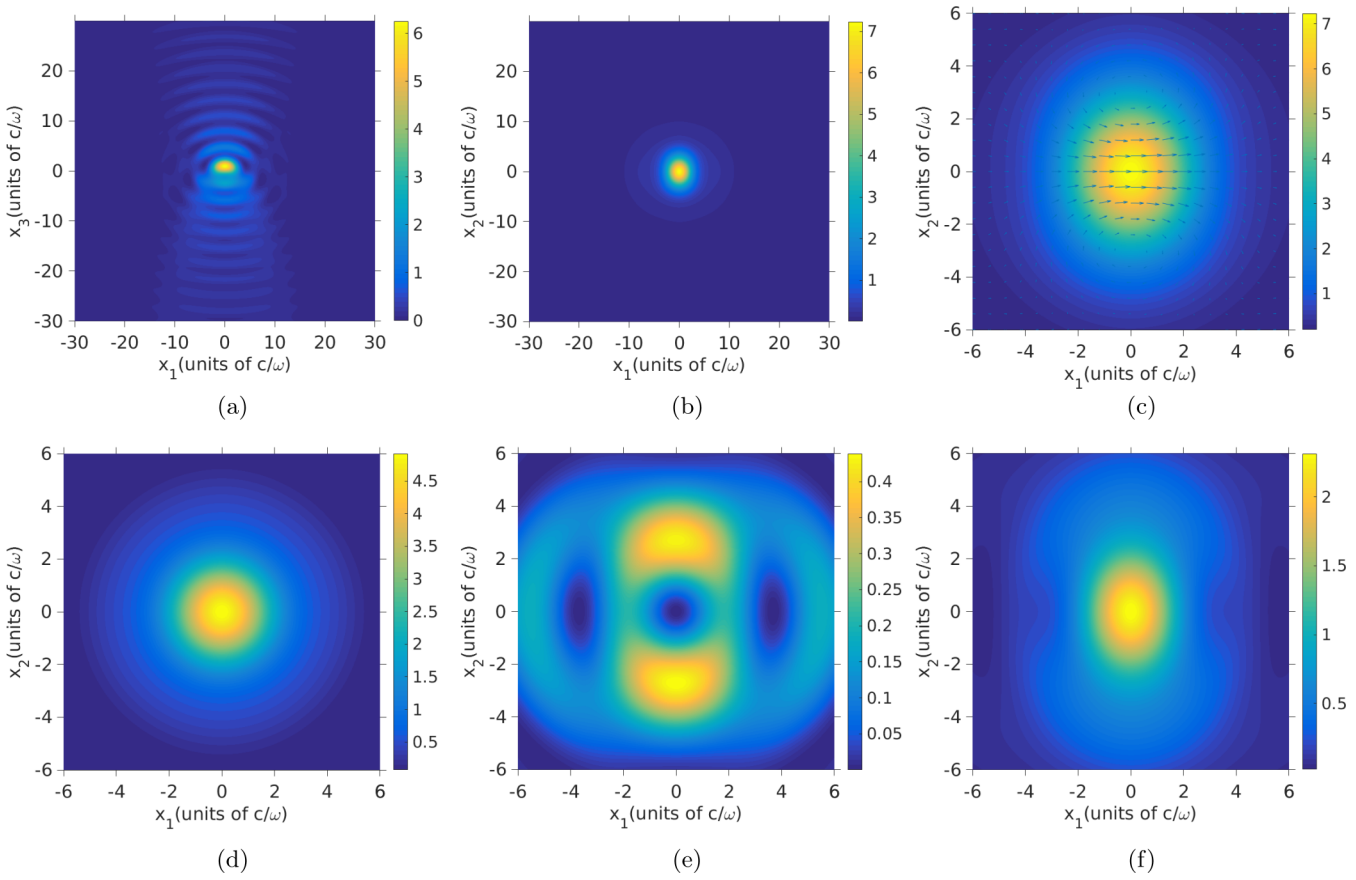

FIG. 5. $\mathcal{E}$ mode with parameters $m = 1, \kappa = 0.032\,372\,77$ and coefficients $c^{(+)}_{\kappa,1} = 1, c^{(-)}_{\kappa,1} = 0$. This κ has the smallest absolute value among the roots of the boundary condition Eq. (93) for a mirror surface at $\zeta_0 = 35\,700c/\omega$. (a),(b) Illustrative example of the em energy density at the planes defined by (a) $x_2 = 0$ and (b) $x_3 = 0$. (c) Electric-field projection into the plane $x_3 = 0$. (d)–(f) Components of the em field at the $x_3 = 0$ plane: (d) $|\mathbf{E} \times \mathbf{e}_3|^2$, (e) $|\mathbf{E} \cdot \mathbf{e}_3|^2$, and (f) $|\mathbf{B} \times \mathbf{e}_3|^2$.

Once again, both sets of coefficients lead to the same electromagnetic mode since a linear combination of them can be found to satisfy Eq. (65).

The $\mathcal{E}$ modes are illustrated in Fig. 5. For the chosen $\mathcal{E}$ mode, the em energy density is mostly of *electric* origin at the focus of the mirror. Three optical vortices are observed for the x_3 component of the electric field at the x_1 axis in Fig. 5(e).

5. $\{\mathbf{E}_\mathcal{B}, \mathbf{B}_\mathcal{B}\}$ *and* $\{\mathbf{E}_\mathcal{E}, \mathbf{B}_\mathcal{E}\}$ *symmetrized elementary modes for* $m < 0$

The results shown for $\mathcal{B}$ modes and $\mathcal{E}$ modes in the previous two sections relied on the identities given in Eqs. (12)–(16) which are valid for $m > 0$. For the $m < 0$ modes, similar results can be obtained by noticing that the solutions of the wave equation for $m < 0$ have a dependence on the ζ and η variables, analogous to that for $m > 0$ but interchanging the role of the functions $V_{\kappa,m\pm1}$ in the components π_+ and π_- of the corresponding Hertz potential.

B. Quantum em field in the presence of a parabolic mirror

The proper characterization of the em modes provides a starting point for a quantum description of light. We have given compact conditions to determine the available modes sustained in the presence of an ideal parabolic mirror by exploiting the symmetries of the em field in such a geometry. From the knowledge of these modes, field quantization can be performed following the prescription used in Sec. III, taking care of the proper normalization of the elementary modes.

In the quantum realm, the electromagnetic field admits the possibility of a plethora of configurations. Each one is determined by the specification of the state of every elementary mode, both for pure and mixed states of the field. In this scheme, the correlation functions characterizing the quantum em field are evaluated with respect to the state each mode is found in (e.g., coherent, squeezed, or number states) multiplied by structure functions that depend on the spatiotemporal distribution of the elementary modes.

As illustrated for the ideal mirror in Figs. 2–5, the modes with small values of $|\kappa|$ exhibit a high degree of 3D localization near the focus of the parabolic mirror. In fact, as already mentioned, the em field of Neuman modes with $|\kappa| \ll 1$ resemble the pattern of the em field radiated by a dipole aligned with the $\mathbf{x}_3$ axis. This observation leads to the following expectative [8]: if an atom in an excited state is located near the focus of a parabolic mirror there is a high possibility that it will emit a single photon naturally described by the Neuman mode with the lowest value of $|\kappa|$ and a frequency compatible with the atomic transition energy. This is in stark contrast with the standard free-space description in terms of plane

waves where an infinite number of possible modes with wave vectors $\vec{k}$ are usually considered. The enhanced atom-em field interaction within a mirror could be used for a deterministic generation of single photons with a given a label or, vice versa, for the control of atomic states through the interaction with photons in a given parabolic mode.

V. DISCUSSION

We have shown that symmetries inherent in a parabolic geometry can be used to obtain closed expressions of the electromagnetic modes in the presence of boundaries exhibiting such geometry. Within the Hertz potentials formalism, these modes incorporate the vectorial character of the em field into the two parameters given by the elementary solutions of the scalar wave equation in a simple way. The intrinsic angular momentum—equivalent to a bivalued parameter $\sigma = \pm 1$—is imprinted on the form of the Hertz potentials: (i) it couples with the orbital angular momentum of the scalar field to yield a vector potential that only involves wave functions with parameters m and $m \pm 1$, and (ii) it modifies the parabolic number κ to yield vector Hertz potentials $\boldsymbol{\pi}^{(m;\kappa)}$ via scalar wave functions with parameters κ and $(2\kappa \pm 1i)/2$; both are shown in Eqs. (58).

The elementary electromagnetic modes encountered from the Hertz potentials exhibit the underlying parabolic symmetry. They are orthonormal with respect to the scalar product defined by an extrapolation of the expression of the em energy density for two different modes, Eq. (63). As a consequence, these modes can be used to quantize the field through the Einstein prescription and define the quantum numbers of the corresponding photons. The quantum numbers are related to dynamical variables of the field and, in turn, its mechanical identity. The m quantum number accounts for the projection of the total angular momentum along the x_3 axis, J_3, and the κ quantum number is half the eigenvalue of the generator $\mathfrak{A}_3$ characteristic of parabolic symmetry. Both numbers could play a dynamical role in matter-em field interactions, the study of which we leave for future work.

The relevance of using symmetrized modes has been further analyzed by working in detail the important case of an ideal parabolic mirror. We have shown that proper boundary conditions can be satisfied by these modes. For a mirror located at ζ_0, the boundary conditions constrain the relative weights of the $\pi_\pm, \pi_0$ components of the vector Hertz potentials and limit the possible values of κ to solutions of the compact expression

$$\mathcal{W}^2_{\kappa,m}(\bar{\zeta}_0) = -\frac{d_+}{d_-}, \quad d_\pm = \frac{1}{2} \pm i\frac{\kappa}{m},$$

which encloses the constrains found for both electric, Eqs. (85) and (97), and magnetic modes, Eqs. (87) and (91). We observed that, even though the boundary condition is naturally written in configuration space, several mathematical manipulations can be dealt with in an easier way in the wave-vector space.

The parabolic em modes exhibit electric and magnetic fields with a nontrivial and rich topology. Regions where electric and magnetic field have different magnitude, phase singularities, vectorial vortices, and strong gradients of the field components are found. These properties should be studied at depth in terms of their effect in the interaction with atomic systems. These properties motivate the study of the effect of light over the external and internal degrees of freedom of material particles.

The experimental generation of any given particular mode is an important subject. A direct implementation corresponds to impinge the boundary conditions on the em field through an accessible surface. In the optical realm the use of space light modulators seems to be a promising option to that end. In fact this idea has already been studied and implemented for Neuman modes by Sonderman *et al.* [8].

The results reported in this paper can also be used to study other interesting configurations, e.g., cavities built from parabolic mirrors. From the analysis reported here, the complete set of modes inside a near confocal cavity bounded by the surfaces $\zeta = \zeta_0$ and $\eta = \eta_0$ is formed by fields with values of the parameter κ that are simultaneous solutions of

$$\mathcal{W}^2_{\kappa,m}(\bar{\zeta}_0) = -\frac{d_+}{d_-}, \quad \mathcal{W}^2_{-\kappa,m}(\bar{\eta}_0) = -\frac{d_-}{d_+}.$$

The feasibility of this condition should be studied in detail; including a comparison with previous works that used the WKB approximation to analyze the em field in confocal cavities [1]. A second example corresponds to explore the use of the symmetrized vectorial em fields in the presence of parabolic lenses.

ACKNOWLEDGMENT

This work was partially supported by CONACyT LN-293471. R.J. thanks G. Leuchs for interesting conversations and L. Sánchez-Soto for stimulating discussions.

APPENDIX A: PARABOLIC COORDINATES AND THE ASSOCIATED SCALE FACTORS

The parabolic coordinates are defined by

$$x_1 = \sqrt{\zeta\eta}\cos\varphi, \quad x_2 = \sqrt{\zeta\eta}\sin\varphi, \quad x_3 = \tfrac{1}{2}(\zeta - \eta) \tag{A1}$$

with

$$0 \leqslant \zeta < \infty, \quad 0 \leqslant \eta < \infty, \quad 0 \leqslant \varphi < 2\pi. \tag{A2}$$

The scale factors are

$$h_\zeta = \frac{1}{2}\sqrt{\frac{\zeta+\eta}{\zeta}}, \quad h_\eta = \frac{1}{2}\sqrt{\frac{\zeta+\eta}{\eta}}, \quad h_\varphi = \sqrt{\zeta\eta}. \tag{A3}$$

The unitary parabolic vectors are

$$\mathbf{e}_\zeta = \sqrt{\frac{\zeta}{\zeta+\eta}}\left[\sqrt{\frac{\eta}{\zeta}}(\cos\varphi\mathbf{e}_1 + \sin\varphi\mathbf{e}_2) + \mathbf{e}_3\right], \tag{A4}$$

$$\mathbf{e}_\eta = \sqrt{\frac{\eta}{\zeta+\eta}}\left[\sqrt{\frac{\zeta}{\eta}}(\cos\varphi\mathbf{e}_1 + \sin\varphi\mathbf{e}_2) - \mathbf{e}_3\right], \tag{A5}$$

$$\mathbf{e}_\varphi = -\sin\varphi\mathbf{e}_1 + \cos\varphi\mathbf{e}_2. \tag{A6}$$

Inverting them one obtains the Cartesian basis:

$$\mathbf{e}_1 = \frac{\sqrt{\eta}}{\sqrt{\zeta+\eta}}\cos\varphi\mathbf{e}_\zeta + \frac{\sqrt{\zeta}}{\sqrt{\zeta+\eta}}\sin\varphi\mathbf{e}_\eta - \sin\varphi\mathbf{e}_\varphi, \quad \text{(A7)}$$

$$\mathbf{e}_2 = \frac{\sqrt{\eta}}{\sqrt{\zeta+\eta}}\sin\varphi\mathbf{e}_\zeta + \frac{\sqrt{\zeta}}{\sqrt{\zeta+\eta}}\sin\varphi\mathbf{e}_\eta + \cos\varphi\mathbf{e}_\varphi, \quad \text{(A8)}$$

$$\mathbf{e}_3 = \frac{\sqrt{\zeta}}{\sqrt{\zeta+\eta}}\mathbf{e}_\zeta - \frac{\sqrt{\eta}}{\sqrt{\zeta+\eta}}\mathbf{e}_\eta. \quad \text{(A9)}$$

Notice that

$$\mathbf{e}_\pm = \mathbf{e}_1 \pm i\mathbf{e}_2 = \frac{e^{\pm i\varphi}}{2}\left[\frac{\mathbf{e}_\zeta}{h_\eta} + \frac{\mathbf{e}_\eta}{h_\zeta} \pm 2i\mathbf{e}_\varphi\right]. \quad \text{(A10)}$$

APPENDIX B: $\mathcal{E}$ MODES IN THE PRESENCE OF AN IDEAL PARABOLIC MIRROR USING PARTIALLY SYMMETRIZED HERTZ POTENTIALS

The use of symmetrized modes allows for compact expressions that describe the em field in the presence of an ideal parabolic mirror. In this appendix, we illustrate the difficulties that arise when solving this problem using vector Hertz potentials that are eigenfunctions of $\hat{J}_3$ but do not necessarily lead to electric and magnetic fields that are eigenfunctions of $\mathfrak{A}_3$. To that end, the boundary conditions are imposed for $\mathcal{E}$ modes generated from partially symmetrized vector Hertz potentials [see Eqs. (47)].

$\{\mathbf{E}_\mathcal{E}, \mathbf{B}_\mathcal{E}\}$ *partially symmetrized modes for* $m = 0$

In this case

$$\pi_\pm^{(0)} = \sum_\kappa c_{\kappa,0}^{(\pm)} e^{\mp i\varphi} V_{\kappa,1}(\bar{\zeta}) V_{-\kappa,1}(\bar{\eta}), \quad \pi_0^{(0)} = \sum_\kappa c_{\kappa,0}^{(0)} V_{\kappa,0}(\bar{\zeta}) V_{-\kappa,0}(\bar{\eta}). \quad \text{(B1)}$$

It can be shown that the condition $p_\eta^{(0)} = 0$ for $\bar{\zeta} = \bar{\zeta}_0$ is satisfied if

$$\left[\sqrt{\bar{\zeta}}\frac{\partial}{\partial\bar{\zeta}}[D_{\kappa,0}^{(+)} - D_{\kappa,0}^{(-)}]\right]\Big|_{\bar{\zeta}=\bar{\zeta}_0} = i\sqrt{\bar{\zeta}}\frac{\partial}{\partial\bar{\zeta}}[(-c_{\kappa+i/2}^{(+)} + c_{\kappa+i/2}^{(-)})V_{\kappa+i/2,1}(\bar{\zeta}) + (c_{\kappa-i/2}^{(+)} - c_{\kappa-i/2}^{(-)})V_{\kappa-i/2,1}(\bar{\zeta})]|_{\bar{\zeta}=\bar{\zeta}_0}, \quad \text{(B2)}$$

with

$$D_{\kappa,0}^{(\pm)} = -i(c_{\kappa+i/2,0}^{(\pm)} V_{\kappa+i/2,0}(\bar{\zeta}) - c_{\kappa-i/2,0}^{(\pm)} V_{\kappa-i/2,0}(\bar{\zeta})).$$

The equation $p_\varphi^{(0)} = 0$ is satisfied if

$$\sum_\kappa [\mu_{\kappa+i}^{(+)} + \mu_\kappa^{(0)} + \mu_{\kappa-i}^{(-)}] V_{-\kappa,m}(\bar{\eta}) = 0, \quad \text{(B3)}$$

and

$$\mu_{\kappa+i}^{(+)} = \left(\frac{1}{2} + i\kappa - 1\right)\left[-\frac{1}{2\sqrt{\bar{\zeta}}}(D_{\kappa+i,0}^{(+)} + D_{\kappa+i}^{(-)}) - D_{\kappa+i,0}^{(0)} - i\frac{\partial D_{\kappa+i,0}^{(0)}}{\partial\bar{\zeta}}\right]\Big|_{\bar{\zeta}=\bar{\zeta}_0},$$

$$\mu_\kappa^{(0)} = \left[\frac{\partial}{\partial\bar{\zeta}}\sqrt{\bar{\zeta}}(D_{\kappa,0}^{(+)} + D_{\kappa,0}^{(-)}) + \frac{1}{2\sqrt{\zeta}}(D_{\kappa,0}^{(+)} + D_{\kappa,0}^{(-)}) + D_{\kappa,0}^{(0)} - 2\kappa D_{\kappa,0}^{(0)}\right]\Big|_{\bar{\zeta}=\bar{\zeta}_0},$$

$$\mu_{\kappa-i}^{(-)} = \left(\frac{1}{2} - i\kappa - 1\right)\left[-\frac{1}{2\sqrt{\bar{\zeta}}}(D_{\kappa-i,0}^{(+)} + D_{\kappa-i,0}^{(-)}) - D_{\kappa-i,0}^{(0)} + i\frac{\partial D_{\kappa+i,0}^{(0)}}{\partial\bar{\zeta}}\right]\Big|_{\bar{\zeta}=\bar{\zeta}_0}.$$

Here

$$D_{\kappa,0}^{(0)} = c_{\kappa,0}^{(0)} V_{\kappa,0}(\bar{\zeta}).$$

These equations involve $D_{\kappa,0}(\bar{\zeta})$ functions with different κ, reflecting the fact that the expression for $\boldsymbol{\pi}^{(0)}$ has not been chosen taking into account the parabolic symmetry generated by $\mathfrak{A}_3$.

$\{\mathbf{E}_\mathcal{E}, \mathbf{B}_\mathcal{E}\}$ *partially symmetrized modes for* $m > 0$

The vectorial Hertz potentials with well defined total angular momentum $\hat{J}_3$ have the structure

$$\pi_\pm^{(m)} = e^{im\varphi}\sum_\kappa c_\kappa^{(\pm)} V_{\kappa,m\mp1}(\bar{\zeta}) V_{-\kappa,m\mp1}(\bar{\eta}), \quad \pi_0^{(m)} = e^{im\varphi}\sum_\kappa c_\kappa^{(0)} V_{\kappa,m}(\bar{\zeta}) V_{-\kappa,m}(\bar{\eta}). \quad \text{(B4)}$$

Using the recurrence relations given by Eqs. (12)–(16), it is possible to write the functions $V_{-\kappa,m\pm1}(\bar{\eta})$ in terms of functions $V_{-\kappa,m}(\bar{\eta})$, so that, according to their definition Eq. (51),

$$P_+^{(m)} = \frac{e^{im\varphi}}{2\sqrt{\bar{\eta}}}\sum_\kappa (D_{\kappa+i/2}^{(+)}(\bar{\zeta}) V_{-\kappa+i/2,m}(\bar{\eta}) + D_{\kappa-i/2}^{(+)}(\bar{\zeta}) V_{-\kappa-i/2,m}(\bar{\eta})), \quad \text{(B5)}$$

$$P_-^{(m)} = \frac{e^{im\varphi}}{\sqrt{\bar{\eta}}}\sum_\kappa (D_{\kappa+i/2}^{(-)}(\bar{\zeta}) V_{-\kappa+i/2,m}(\bar{\eta}) + D_{\kappa-i/2}^{(-)}(\bar{\zeta}) V_{-\kappa-i/2,m}(\bar{\eta})), \quad \text{(B6)}$$

with

$$D^{(+)}_{\kappa\pm i/2}(\bar{\xi}) = c^{(+)}_{\kappa} V_{\kappa,m-1}(\bar{\xi})\left(-\frac{1}{2} \mp \frac{i\kappa}{m}\right) + c^{(-)}_{\kappa} V_{\kappa,m+1}(\bar{\xi})[\mp i(|m|+1)],$$
$$D^{(-)}_{\kappa\pm i/2}(\bar{\xi}) = c^{(+)}_{\kappa} V_{\kappa,m-1}(\bar{\xi})\left(-\frac{1}{2} \mp \frac{i\kappa}{m}\right) - c^{(-)}_{\kappa} V_{\kappa,m+1}(\bar{\xi})[\mp i(|m|+1)]. \tag{B7}$$

Since Eqs. (B5) and (B6) involve the functions $V_{-\kappa\pm i/2,m}(\bar{\xi})$, it is suggested to write

$$\pi_0^{(m)} = e^{im\varphi} \sum_{\kappa} \tilde{d}^{(0)}_{\kappa+i/2} V_{-\kappa-i/2,m}(\bar{\eta}) + \tilde{D}^{(0)}_{\kappa-i/2} V_{-\kappa+i/2,m}(\bar{\eta}), \quad \tilde{D}^{(0)}_{\kappa\pm i/2} = c^{(0)}_{\kappa\pm i/2} V_{\kappa\pm i/2}(\bar{\xi}). \tag{B8}$$

This expression should lead to results compatible with those obtained from fully symmetrized modes for each κ value. Within the analysis presented in this appendix the interpretation of κ is not direct. Even more if the ansatz Eq. (B8) is not made and one insists on working with the general expression for $\pi_0^{(m)}$, the following hierarchy of equations is found:

$$\sum_{\kappa} \left(\lambda^{3/2}_{-\kappa+3i/2} V_{-\kappa+3i/2,m} + \lambda^{1/2}_{-\kappa+i/2} V_{-\kappa+i/2,m} + \lambda^{-1/2}_{-\kappa-i/2} V_{-\kappa-i/2,m} + \lambda^{-3/2}_{-\kappa-3i/2} V_{-\kappa-3i/2,m}\right) = 0, \tag{B9}$$

under the definitions

$$\lambda^{3/2}_{-\kappa+3i/2} = \left(-i\tilde{c}^{(0)}_{\kappa-i/2} + \frac{\sqrt{\bar{\xi}}}{2}\frac{\partial}{\partial\bar{\xi}} D^{(-)}_{\kappa+i/2}\right)\left(\frac{|m|+1}{2} - i(\kappa+i/2)\right),$$
$$\lambda^{1/2}_{-\kappa+i/2} = \frac{1}{2}\frac{\partial}{\partial\bar{\xi}}\sqrt{\bar{\xi}} D^{(+)}_{\kappa+i/2,m} - 2(\kappa+i/2)\tilde{c}^{(0)}_{\kappa-i/2} - \frac{1}{2}\frac{\sqrt{\bar{\xi}}}{2}\frac{\partial}{\partial\bar{\xi}} D^{(-)}_{\kappa+i/2} + \left(\frac{|m|+1}{2} - i(\kappa-i/2)\right)\left(-i\tilde{c}^{(0)}_{\kappa+i/2} + \frac{1}{2}\frac{\sqrt{\bar{\xi}}}{2}\frac{\partial}{\partial\bar{\xi}} D^{(-)}_{\kappa-i/2}\right),$$
$$\lambda^{-1/2}_{-\kappa-i/2} = \frac{1}{2}\frac{\partial}{\partial\bar{\xi}}\sqrt{\bar{\xi}} D^{(+)}_{\kappa-i/2,m} - 2(\kappa-i/2)\tilde{c}^{(0)}_{\kappa+i/2} - \frac{1}{2}\frac{\sqrt{\bar{\xi}}}{2}\frac{\partial}{\partial\bar{\xi}} D^{(-)}_{\kappa-i/2} + \left(\frac{|m|+1}{2} + i(\kappa+i/2)\right)\left(+i\tilde{c}^{(0)}_{\kappa-i/2} + \frac{1}{2}\frac{\sqrt{\bar{\xi}}}{2}\frac{\partial}{\partial\bar{\xi}} D^{(-)}_{\kappa+i/2}\right),$$
$$\lambda^{-3/2}_{-\kappa-3i/2} = \left(-i\tilde{c}^{(0)}_{\kappa+i/2} - \frac{\sqrt{\bar{\xi}}}{2}\frac{\partial}{\partial\bar{\xi}} D^{(-)}_{\kappa-i/2}\right)\left(\frac{|m|+1}{2} + i(\kappa-i/2)\right). \tag{B10}$$

For $\{\mathbf{E}_{\mathcal{E}}, \mathbf{B}_{\mathcal{E}}\}$, and $m < 0$ the role of the functions π_+ and π_- is interchanged, since the $V_{\kappa,m}$ functions defined in Eq. (11) involve the absolute value of m.

APPENDIX C: PARABOLIC MIRROR BOUNDARY CONDITION IN TERMS OF COULOMB FUNCTIONS

Under standard conditions, the natural lengths describing the mirror (e.g., focal length and size) are much greater than the wavelengths of the em fields of interest. In order to facilitate the numerical evaluation of the values of κ satisfying Eq. (93) in this regime, it is necessary to study the asymptotic behavior of the $\mathcal{W}_{\kappa,m}(\bar{\xi}_0)$ function. In this appendix, we perform such an analysis in two steps. First, we write the $V_{\kappa\pm i/2,m}(\bar{\xi}_0)$ function in terms of Coulomb functions, Eq. (20). Second, we use the asymptotic expressions for those functions [14].

Let us define

$$\mathcal{F}_{\kappa,m}(\bar{\xi}_0) = \frac{F_{(|m+1|-1)/2}(\kappa, \bar{\xi}_0/2)}{F_{(|m-1|-1)/2}(\kappa, \bar{\xi}_0/2)}, \tag{C1}$$

for m a nonzero even integer. Using Eqs. (12) and (13) it results that

$$\mathcal{F}_{\kappa,m}(\bar{\xi}_0) = -i\frac{(V_{\kappa+i/2,m} - V_{\kappa-i/2,m})|d_+|}{d_+ V_{\kappa-i/2,m} + d_- V_{\kappa+i/2,m}} = -i\frac{(\mathcal{W}_{\kappa,m} - 1)|d_+|}{d_+ + d_- \mathcal{W}_{\kappa,m}}. \tag{C2}$$

By inverting this equation

$$\mathcal{W}_{\kappa,m} = \frac{|d_+| + i\mathcal{F}_{\kappa,m} d_+}{|d_-| - i\mathcal{F}_{\kappa,m} d_-}, \tag{C3}$$

the boundary condition

$$\mathcal{W}^2_{\kappa,m} = -\frac{d_+}{d_-} \tag{C4}$$

is shown to be equivalent to

$$\mathcal{F}^2_{\kappa,m}(\bar{\xi}_0) = 1. \tag{C5}$$

There is an infinite number of roots $\{\kappa_0\}$ of this equation. In fact, for $\bar{\xi}_0 \gg \kappa$ an analytical result can be given. In this case, and for $m > 0$, the boundary condition can be approximated by

$$\frac{\cos^2\theta_{\kappa,m}}{\tan^2\varphi_{\kappa,m}}[1 - \tan^2\varphi_{\kappa,m} - 2(\tan\theta_{\kappa,m})(\tan\varphi_{\kappa,m})] \sim 0 \tag{C6}$$

with

$$\theta_{\kappa,m} = \arctan(2\kappa/m);$$
$$\varphi_{\kappa,m} = \frac{\bar{\xi}_0}{2} - \kappa\ln\bar{\xi}_0 - \frac{|m|}{2}\frac{\pi}{2} + \arg\Gamma(md_+).$$

Notice that $(2\ell+1)\pi = 2\theta_{\kappa_\ell,m}$, with ℓ an integer number, guarantees the fulfillment of Eq. (C6) but yields a divergent root κ_0 that breaks the condition $\bar{\xi}_0 \gg \kappa$.

[1] J. U. Nöckel, G. Bourdon, E. Le Ru, R. Adams, I. Robert, J.-M. Moison, and I. Abram, Mode structure and ray dynamics of a parabolic dome microcavity, Phys. Rev. E **62**, 8677 (2000).

[2] G. Alber, J. Z. Bernád, M. Stobińska, L. L. Sánchez-Soto, and G. Leuchs, QED with a parabolic mirror, Phys. Rev. A **88**, 023825 (2013).

[3] G. Zumofen, N. M. Mojarad, V. Sandoghdar, and M. Agio, Perfect Reflection of Light by An Oscillating Dipole, Phys. Rev. Lett. **101**, 180404 (2008).

[4] V. Leong, M. A. Seidler, M. Steiner, A. Cerè, and C. Kurtsiefer, Time-resolved scattering of a single photon by a single atom, Nat. Commun. **7**, 13716 (2016).

[5] M. Cray, M.-L. Shih, and P. W. Milonni, Stimulated emission, absorption, and interference, Am. J. Phys. **50**, 1016 (1982).

[6] H. Paul and R. Fischer, Light absorption by a dipole, Sov. Phys. Usp. **26**, 923 (1983).

[7] S. J. van Enk and H. J. Kimble, Strongly focused light beams interacting with single atoms in free space, Phys. Rev. A **63**, 023809 (2001).

[8] M. Sondermann, R. Maiwald, H. Konermann, N. Lindlein, U. Peschel, and G. Leuchs, Design of a mode converter for efficient light-atom coupling in free space, Appl. Phys. B **89**, 489 (2007).

[9] R. Dorn, S. Quabis, and G. Leuchs, Sharper Focus for a Radially Polarized Light Beam, Phys. Rev. Lett. **91**, 233901 (2003).

[10] D. Pinotsi and A. Imamoglu, Single Photon Absorption by a Single Quantum Emitter, Phys. Rev. Lett. **100**, 093603 (2008).

[11] T. Wilk, S. C. Webster, A. Kuhn, and G. Rempe, Single-atom single-photon quantum interface, Science **317**, 488 (2007).

[12] S. A. Aljunid, M. K. Tey, B. Chng, T. Liew, G. Maslennikov, V. Scarani, and C. Kurtsiefer, Phase Shift of a Weak Coherent Beam Induced by a Single Atom, Phys. Rev. Lett. **103**, 153601 (2009).

[13] C. P. Boyer, E. G. Kalnins, and W. Miller Jr., Symmetry and separation of variables for the Helmholtz and Laplace equations, Nagoya Math. J. **60**, 35 (1976).

[14] M. Abramowitz and I. Stegun, *Handbook of Mathematical Functions* (US National Bureau of Standards, Washington, DC, 1964).

[15] W. Pauli, Z. Phys. **36**, 336 (1926); reprinted in *Sources of Quantum Mechanics*, edited by B. L. van der Waerden (Dover, New York, 1968).

[16] M. Bander and C. Itzykson, Group theory and the hydrogen atom, Rev. Mod. Phys. **38**, 330 (1966).

[17] A. P. Prudnikov, Yu. A. Brychov, and O. I. Marichev, *Integrals and Series* (Gordon and Breach, New York, 1986), Vol. 2.

[18] I. S. Gradshteyn and I. M. Ryzhik, *Table of Integrals, Series, and Products* (Academic Press, San Diego, 1965).

[19] A. Nisbet, Hertzian electromagnetic potentials and associated gauge transformations, Proc. R. Soc. London, Ser. A **231**, 250 (1955).

[20] J. M. Jauch and F. Rohrlich, *Theory of Photons and Electrons* (Springer-Verlag, New York, 1955).

[21] R. Jáuregui and S. Hacyan, Quantum-mechanical properties of Bessel beams, Phys. Rev. A **71**, 033411 (2005).

[22] B. M. Rodríguez-Lara and R. Jáuregui, Dynamical constants for electromagnetic fields with elliptic-cylindrical symmetry, Phys. Rev. A **78**, 033813 (2008).

[23] B. M. Rodríguez-Lara and R. Jáuregui, Dynamical constants of structured photons with parabolic-cylindrical symmetry, Phys. Rev. A **79**, 055806 (2009).

[24] C. L. Hernández-Cedillo, S. Bernon, H. Hattermann, J. Fortágh, and R. Jáuregui, Scattering of dilute thermal atom clouds on optical Weber beams, Phys. Rev. A **87**, 023404 (2013).

[25] H. He, N. R. Heckenberg, and H. Rubinsztein-Dunlop, Optical particle trapping with higher-order doughnut beams produced using high efficiency computer generated holograms, J. Mod. Opt. **42**, 755 (1995).